Heteroatom Chemistry
Volume 18, Number 2, 2007

What Can We Learn from Two-Center Three-Electron Bonding with the Topological Analysis of ELF?

I. Fourré and B. Silvi

Laboratoire de Chimie Théorique (UMR-CNRS 7616), Université Pierre et Marie Curie, 4 Place Jussieu, 75252 Paris cédex, France

Received 18 October 2005; revised 17 November 2005

ABSTRACT: *In this paper, a review is presented of the abundant literature on the two-center three-electron (2c-3e) bonding, which plays a crucial role in electron transfer and radical chemistry. Important questions regarding this peculiar type of interaction are (1) Is a three-electron bonded complex a molecule or an assembly of molecules?, (2) Since an unpaired electron is involved, where is the spin density located?, and (3) Is there a descriptor of electron fluctuation, which is a central phenomenon in this type of bonding? We demonstrate that the topological analysis of the electron localization function (ELF), which provides a convenient mathematical framework to study chemical bond in molecules and solids, is able to answer these questions. First, examples of potentially 3e-bonded complexes proposed by Pauling are reinvestigated. Second, the electron attachment process on molecules of the* H_nXYH_m *type with X,Y = Cl, S, P, Si and* n, m = *0–2 is considered. Finally, the ELF-based topology of some prototypical radicals containing the SO bond is examined. From these studies, several topological signatures of the 3e bonding have been elaborated. No disynaptic basin, well known as the topological signature of a covalent shared-electron pair interaction, is found between two 3e-bonded atoms. Therefore, to distinguish 3e bonds from ionic or hydrogen bonds, a core valence bifurcation (CVB) index has been introduced, similar to the one previously defined by Fuster and Silvi (Theor Chem Acc 2000,104,13) to differentiate weak and medium H-bonds. Moreover, in 3e-bonded systems, the spin density is mainly localized within the lone-pair basins of the heavy atoms. To quantify the electron fluctuation, a topological delocalization index has been defined. An unambiguous characterization of the 3e bonding is thus obtained, which is in agreement with other theoretical approaches, such as the valence bond method.*
 Heteroatom Chem 18:135–160, 2007; Published online in Wiley InterScience (www.interscience.wiley.com). DOI 10.1002/hc.20325

INTRODUCTION

Two-center three-electron (2c-3e) bonded radicals, which are characterized by a relatively weak bond between two heteroatoms, have attracted considerable attention in recent years. They are important because they act as reaction intermediates during electron transfer processes, in particular, in biological environments. They were initially described in 1931 by Pauling in one of his classical papers on the nature of the chemical bond [1] and later in his book [2].

What Is Two-Center Three-Electron Bonding?

In the valence-bond (VB) formalism, 2c-3e bonds owe their stabilities to a resonance between two Lewis structures that are mutually related by charge

Correspondence to: I. Fourré; e-mail: fourre@lct.jussieu.fr.

transfer as shown in (1), (2), and (3) for 3e-bonded cation, anion, and neutral radicals, respectively.

$$A^{\bullet +} : B \leftrightarrow A : {}^{\bullet}B^{+} \quad (1)$$

$$A^{\bullet} : B^{-} \leftrightarrow A :^{-} {}^{\bullet}B \quad (2)$$

$$A^{\bullet} : B \leftrightarrow A :^{-} {}^{\bullet}B^{+} \quad (3)$$

In these resonance situations, the energy difference ΔE between the two limiting structures must be small enough to achieve a sizeable stabilization energy [3]. For cationic radicals, ΔE is the difference in ionization potentials (IP) of species A and B. For anion radicals, it is the difference in electron affinity (EA) and for neutral radicals it is the difference in IP of B and EA of A. This explains why the three-electron bond occurs mainly in homodimeric ionic systems and more rarely in neutral ones, at least in the gas phase. In molecular orbital (MO) terms, a closed shell orbital, typically a lone pair of one fragment A, interacts with the singly occupied MO of the B fragment, resulting in a doubly occupied bonding MO (usually a σ orbital) and a singly occupied antibonding MO (σ^*) of the composite molecule A$\therefore$B, as depicted in Fig. 1, where the eventual charge of the fragment and of the radical has been omitted for the sake of simplicity. To form a stable 2c-3e bond, the interacting fragment MOs must be close in energy, similar to the requirement of small ΔE in the VB model. Furthermore, the fragments that are linked in such a bond, one cation and one neutral for a 3e-bonded cation radical (respectively one neutral and one anion for a 3e-bonded radical anion), must each bear a lone pair, which is singly occupied in the cation (respectively in the neutral) and doubly occupied in the neutral fragment (respectively in the anion fragment). All molecules of the generic form XR_n (R being H or a substituent) with (X,n) = (Ne or He, O), (F,1), (O,2), (N,3) (respectively with (X,n) = (F,1), (O,2), (N,3)) and their second-row analogues are therefore candidates for forming three-electron bonds with cations (respectively with anions) of the same set. Generally the strongest 3e bonds associate two identical fragments. In summary, these bonds occur mainly between rare gas atoms or heteroatoms of the first and second periods, hence He$\therefore$He, N$\therefore$N, O$\therefore$O, F$\therefore$F, Ne$\therefore$Ne, P$\therefore$P, S$\therefore$S, Cl$\therefore$Cl, and Ar$\therefore$Ar constitute typical 2c-3e bonds. The dihalogen anions, as well as the rare gas cation dimers, constitute prototype 2c-3e bonded systems. Since the bond order in such a molecule will be one half (thus the name "hemibonds" sometimes given to these types of bonds), the dissociation energy will be roughly half of the corresponding two-electron bond and the bond distance will be longer. It is worthwhile to mention that one-electron bonds, though outside the scope of this paper, are also classified as "hemibonds" because a single electron occupies the bonding orbital (examples are given by H_2^+ and the dialkali metal radical cations). However, the 2c-3e bonds are generally weaker than the 2c-1e bonds, because of the greater destabilization caused by the antibonding electron with respect to the stabilization caused by the bonding electron.

Some Examples of 2c-3e Bonded Complexes Proposed by Pauling

In his fundamental paper [2], Pauling examined several examples of 3e-bonded species, the simplest one being He_2^+. He also proposed the nitric oxide radical NO, which is the most stable of the odd-electron molecules, and presents a partial 2c-3e bonding character. In his opinion, it involves a double bond plus a three-electron bond between the two atoms, resulting from the resonance between the structures I and II shown in Fig. 2. This may explain why NO does not polymerize in the gas phase. The existence of the hemibond implies a delocalized electron between N and O, whereas dimerization would

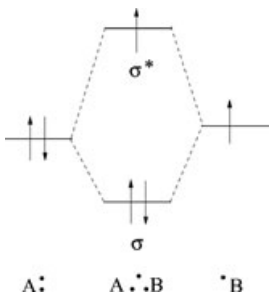

FIGURE 1 Molecular orbital diagram for the A$\therefore$B three-electron bond showing the two bonding electrons in the (σ) orbital and the antibonding electron in the (σ^*) orbital.

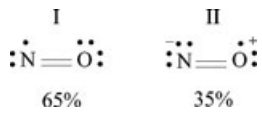

FIGURE 2 The two Lewis resonant structures proposed by Pauling for the NO molecule.

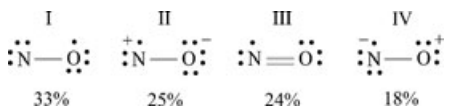

FIGURE 3 The four Lewis resonant structures inferred from the ELF description of NO (see text).

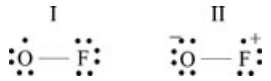

FIGURE 4 The two Lewis resonant structures proposed by Pauling for the OF molecule.

require the localization of the odd-electron on the nitrogen atom. Another example given by Pauling is the nitrogen dioxide (NO_2) in which one oxygen is attached to nitrogen by a double bond and one by a single bond plus a three-electron bond. The simple dioxygen molecule, containing two unpaired electrons and being consequently strongly paramagnetic, is better described by a single bond and two three-electron π-bonds rather than by a double bond. The structure of the superoxide ion O_2^- has been determined by the measurement of the magnetic susceptibility of the highest oxide of potassium, KO_2 [4]: the crystal is supposed to contain O_2^- ions in a $^2\Pi$ state, involving a single bond and a 3e bond. Among the other molecules proposed by Pauling as candidates for 2c-3e bonded compounds, several involve the halogen atoms: for example, OF, ClO_2 [5], and Cl_2^-. The two neutral radicals are actually partially 3e-bonded species. The former is described by a single bond and a three-electron bond, as in Fig. 4, whereas in the latter one oxygen atom is attached by a single bond to chlorine, while the other is held by a single bond plus a three-electron bond, as in Fig. 5. In contrast to the preceding examples, Cl_2^- is a pure 3e-bonded radical anion, i.e., its stability is only due to the resonance 1 with A=B=Cl.

Recent Experimental and Theoretical Studies of 2c-3e Bonded Complexes

Three-electron bonds are encountered in many different areas such as free-radical chemistry in solution [6–11], as well as in gas [12–15], and solid phases [16], biochemistry [17–23], organic reactions [24–26], radiation studies [27–30], intrazeolite chemistry [31,32], bioinorganic enzymology [33–35], and are preferentially observed in cations. The most extensively studied group is that of sulfur-centered radical cations, but they can also be found in anions [7,21,25,26,29] or neutrals adducts [24,27,28,30,36]. Time-resolved pulse radiolysis techniques have demonstrated that particularly the sulfur-containing species exhibit strong optical absorption in the visible and near UV regions. On the basis of the results obtained for various sulfur-containing 3e-bonded radicals, these optical absorptions were, in the first approximation, attributed to $\sigma \rightarrow \sigma^*$ transition [6]. In general, three-electron bonds are formed intermolecularly, for example, between a sulfur radical cation and the sulfur atom of another molecule, but they can also exist intramolecularly, if two [10] or more [16] sulfur atoms are located in the same molecule. In this latter case, a novel radical cation having a 2,3,5,6-tetrathiabicyclo[2.2.2]oct-7-ene structure has been characterized by X-ray spectroscopy. Its remarkable stability is attributed to resonance between two limiting structures, each of them constitutes a 2c-3e bond between two sulfur atoms belonging to two different disulfide linkages. Intramolecular N$\therefore$S and S$\therefore$O bonds are also frequently formed, for example, during the process of oxidation of sulfur in methionine or methionine-containing peptides. This process plays an important role during pathologic conditions associated with oxidative stress [22,23,37,38]. It has also been observed by means of femtosecond spectroscopy between the two nitrogen atoms of excited 1,8-bis(dimethylamino)naphthalene, a molecule that combines a strong basicity with a low-nucleophilic character and is known as the prototype of organic "proton sponges" [30]. It is worth noting that competition can occur between two-center three-electron bonds and hydrogen bonding, as suggested by theoretical studies [39], further supported, for example, by ion/molecule association reactions in mixtures of methyl halide and dimethyl sulfide studied by mass spectrometry [14]. The competitive formation of σ (i.e., 2c-3e)-type or π-type bonding has also been evidenced in the photochemical one-electron oxidation of aromatic sulfides [40] and has been shown to be sensitive to the steric and electronic influence of substituents. Finally, although it is formally out of the scope of heteroatom chemistry, 3e bonds involving metal atoms exist: the ferryl group Fe=O in di-iron enzymes core models [41], the Al$\therefore$N or the Al$\therefore$C bonds that are formed spontaneously after insertion of the Al atom into alkyl ethers [42] or into the NH_3 molecule [43], and the

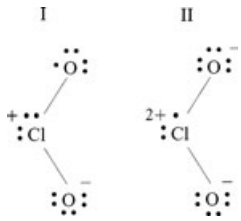

FIGURE 5 The Lewis resonant structures proposed by Pauling for the ClO_2 molecule, showing the 2c-3e bond between the chlorine atom and the "up" oxygen atom. The complete resonant scheme involves two other similar structures (I′ and II′), taking into account the electron delocalization between the two equivalent oxygen atoms and showing the 2c-3e bond between Cl and the "down" oxygen atom.

Rh∴Rh bond [44] or Rh∴Ir bond [45] in bridged complexes, which have been evidenced by X-ray structural studies.

From a theoretical point of view, the most frequently studied species are the rare gas dimer cations [46,47], dihalogen anions [48–50], and disulfide ions [51–55], which have long been experimentally identified. In two landmark papers, Clark [3] and Gill and Radom [39] investigated all the model systems of the type $H_mX\therefore YH_n^+$, attempting to rationalize the existence of 2c-3e bonds. In particular, Gill and Radom found that high level of *ab initio* theory including electron correlation is essential to predict correct dissociation energies. As far as methodology is concerned, the reasons why the description of odd-electron bonding by Hartree–Fock (HF) theory is physically wrong have been clearly explained by Hiberty et al. [56]. Indeed, the crucial feature of this bonding is electron fluctuation, i.e., resonance between charge-shifted related structures, as shown by the VB descriptions (1), (2), and (3) of 3e-bonded cation, anion, and neutral radicals, respectively. A correct description of this phenomenon should allow the orbitals to adapt in size and shape in response to this charge fluctuation, which is formally impossible to obtain in the framework of the HF theory. For dissymmetric X∴Y bonds, it can result in a erroneous sharing of the charge, i.e., of the spin density between the two atoms. A simple nonempirical remedy, using the breathing orbital valence bond (BOVB) method [57], has been proposed which corrects the dissociation energy that was found to be too small. Concerning density functional theories, some of the most popular, in particular those based on Becke's exchange functionals, have demonstrated to systematically overestimate 2c-3e bond dissociation energies, whereas bond lengths are found to be too long and frequencies too low [53,58–61]. The problem lies in overestimating the self-interaction energy in the description of delocalized states. For the ground state of the $(H_2O)_2^+$ radical cation, modern density functionals favor the 3e-bonded structure, whereas correlated calculations show the proton-transferred isomer to be the most stable [59,62]. Only the BH&HLYP functional, which includes 50% HF exchange, 50% Becke exchange, and the additional correlation effects of the LYP functional [63], performs surprisingly well for 2c-3e bonded cation radicals, except for the rare gas dimers and for some 2c-3e bonded radical anions. Some attempts have been made to improve the description of the dissociation of these bonds by Density Functional Theory (DFT) [60,64–66]. For example, Jaramillo and Scuseria proposed a new local hybrid functional scheme with position-dependent amounts of exact exchange that partially corrects the self-interaction error and improves significantly dissociation energies and equilibrium distances [64]. Among the post-HF approaches, the second-order Moller–Plesset (MP2) method has been used for numerous cationic [3,39], anionic [67], and neutral radicals [68,69]. This method appears to be the only candidate for calculating chemical properties of hemibonded species, since it includes the essential dynamical correlation at a rather economical cost, provided the molecules are symmetric and the geometries that are considered are not too stretched relative to equilibrium [50,70]. Numerous other methodological analyses have been published that provided better insight into the nature of this peculiar type of bonding either in cationic [51,52,71,73], anionic [74–76], or neutral species [68,69,78,79]. The crucial problem of competition that often occurs between 2c-3e bonded and hydrogen-bonded species and may determine the stability of the former has also been addressed in several studies [80–82]. Finally, in connection to some previously mentioned experimental papers, there is a growing interest for the theoretical investigations of the 2c-3e S∴O bond that could stabilize the sulfide radical cations in biological environment [83,86].

Objectives of This Paper

In contrast to several previously mentioned theoretical publications, our aim is not to provide precise equilibrium distances, dissociation energies, nor vibrational frequencies of 2c-3e bonds, but rather to investigate the nature of these bonds by means of topological tools, which determine the qualitative characteristics of this type of bonding. In particular, we try to answer the following questions:

i. Is a three-electron bonded complex a molecule or an assembly of molecules?
ii. Since an unpaired electron is involved, where is located the spin density?
iii. Is there a topological descriptor of electron fluctuation, which is a central phenomenon in this type of bonds?

To achieve this goal, highly accurate wavefunctions are generally useless. However, the calculations should give rise to the following: (i) correct electronic state, (ii) a geometry in agreement with the available experimental results or those of the best calculations (a few percent of angstroms on the distances and a few degrees on the angles are sufficient), and (iii) the order of magnitude of the dissociation energy. The topological analysis of the

electron localization function (ELF) of Becke and Edgecombe [87] analyzes density functions, which are extracted, in the majority of cases from MO wavefunctions, although they could, in principle, be applied to densities obtained from VB wavefunctions or to experimental densities. We will demonstrate in this article that the ELF approach is able to provide a description a 2c-3e bonded molecules in terms of "topological signatures." Belonging to the group of topological theories of chemical bonding pioneered by Bader in his atoms-in-molecules (AIM) method [88], the topological analysis of ELF aims to partition the molecular space into chemically significant regions, thus providing a mathematical model of the Lewis theory. During the last 10 years, it has been mainly developed in our laboratory [89–95] and has been extensively applied by numerous groups to the understanding of the chemical structure of molecules [77,79,96,97–122] and solids [123,124]. It has also been combined with the catastrophe theory, a theory of chemical reactions, in which the evolution of ELF is studied as a function of control parameters [125–129].

The organization of this paper is as follows: the following section is devoted to the foundations of the topological analysis of ELF. Later, several textbook examples of Pauling [2] are examined, such as the prototypical cation dimer He_2^+, to which we added Ne_2^+. This enables us to verify that the topology of 2c-3e bonded molecules does not depend on the method employed to calculate the wavefunction, and to give a primary topological description of 2c-3e bonded molecules. We also consider three neutral radicals, namely NO, OF and, ClO_2, which should present, according to Pauling, a partial 2c-3e bond character. The nature of the X—O bond (X = N,F,Cl) is discussed into the framework of the ELF analysis and the resonant schemes which are inferred are compared to the ones of Pauling. Subsequent sections are devoted to the most striking results previously obtained into two different works; the first one deals with the process of electron attachment anion $H_nX\therefore YH_m^-$ series (X,Y = heteroatom of the second period and $n = 0,1,2,3$) [77], whereas the second one is a comparative study of the SO bond in prototypical radicals, ionic and neutral, $RSOH^-$, $RR'SOH_2^+$, and RR′SOH with R,R′ = H,CH_3 [79]. These complementary studies allow us to determine unambiguous topological signatures of the 2c-3e bond.

A SKETCH OF THE ELF ANALYSIS

The aim of the method is to provide a mathematically sound framework enabling a partition of the three-dimensional coordinate space in adjacent regions, fulfilling as well as possible a one-to-one correspondence with the chemical objects of Lewis' valence theory [130,131]. The gradient dynamical system theory (see Abraham and Marsden [132,133]) has already been successfully demonstrated to be a reliable and appropriate tool in the context of Richard Bader's AIM theory [88]. Consider a local function, $\eta(\mathbf{r})$, called the potential function in the dynamical system theory context. This local function carries the chemical information, whereas its gradient $\Delta\eta(\mathbf{r})$ forms a vector field bounded on $\mathbb{R}^3$. This vector field determines two types of points of $\mathbb{R}^3$: the wandering points at which $\Delta\eta(\mathbf{r}_w) \neq 0$ and the critical points which correspond to $\Delta\eta(\mathbf{r}_c) = 0$. The critical points are characterized by their index which is the number of positive eigenvalues of the second derivative (Hessian) matrix of $\eta(\mathbf{r})$. The formal analogy with a velocity field (i.e., $\Delta\eta(\mathbf{r}) = d\mathbf{r}/dt$) enables one to build trajectories by integrating over the time variable. Each trajectory starts in the neighborhood of a point (or set of points) for which $\Delta\eta(\mathbf{r}) = 0$, called the α-limit, and ends in the neighborhood of another point (or set of points) for $\Delta\eta(\mathbf{r}) = 0$, called the ω-limit. Except for asymptotic behavior, the α- and ω-limits are critical points. The set of trajectories having a given critical point as ω-limit is called the stable manifold of this critical point, whereas its unstable manifold is the set of trajectories for which it is a α-limit. The stable manifold of a critical point of index 0 (a local maximum or *attractor*) is the basin of the attractor, that of a critical point of index larger than 0 is a separatrix: it is the boundary between basins.

As already mentioned, it is the potential function $\eta(\mathbf{r})$ that provides the chemical information. Becke and Edgecombe's electron localization function [87,92,134,135] is derived from the measure of the Fermi hole curvature and interpreted in terms of local excess kinetic energy due to Pauli repulsion. It is confined to the [1,0] interval in order to tend to 1 where parallel spins are highly improbable, and where there is therefore a high probability of opposite spin pairs, and to zero in regions where there is a high probability of same spin pairs. Another local descriptor of the pair formation in the sense of Lewis's model, the so-called spin pair composition, has recently been introduced on the basis of the two-particle probability density analysis [92]. This function is defined as the ratio of same spin- and opposite spin-pair functions integrated over a sampling volume around the reference point:

$$c_\pi(\mathbf{r}) = \bar{N}(\mathrm{r})^{-2/3}\frac{\bar{N}_\parallel(\mathbf{r})}{\bar{N}_\perp(\mathbf{r})} \tag{4}$$

with

$$\bar{N}(\mathbf{r}) = \int_V \rho(\mathbf{r}_1)\,\mathrm{d}\mathbf{r}_1$$

$$\bar{N}_{\parallel}(\mathbf{r}) = \int_V\int_V \pi^{\alpha\alpha}(\mathbf{r}_1,\mathbf{r}_2)\,\mathrm{d}\mathbf{r}_1\,\mathrm{d}\mathbf{r}_2 + \int_V\int_V \pi^{\beta\beta}(\mathbf{r}_1,\mathbf{r}_2)\,\mathrm{d}\mathbf{r}_1\,\mathrm{d}\mathbf{r}_2$$

$$\bar{N}_{\perp}(\mathbf{r}) = \int_V\int_V \pi^{\alpha\beta}(\mathbf{r}_1,\mathbf{r}_2)\,\mathrm{d}\mathbf{r}_1\,\mathrm{d}\mathbf{r}_2 + \int_V\int_V \pi^{\beta\alpha}(\mathbf{r}_1,\mathbf{r}_2)\,\mathrm{d}\mathbf{r}_1\,\mathrm{d}\mathbf{r}_2 \tag{5}$$

In these equations, $\rho(\mathbf{r})$ is the spinless one-electron density distribution function, and $\pi^{\sigma\sigma'}(\mathbf{r}_1,\mathbf{r}_2)$ denotes the $\sigma\sigma'$ component of the two-particle distribution $\pi(\mathbf{r}_1,\mathbf{r}_2)$, with $\sigma,\sigma' = \alpha,\beta$. It has been shown that ELF is an excellent approximation to this function, once put in the Lorentzian form $\eta(\mathbf{r}) = (1+c_\pi^2(\mathbf{r}))^{-1}$. ELF has the advantage that it can be expressed analytically in terms of basis functions, in all practical cases where the wavefunction is expressed in terms of orbitals, whereas the spin pair composition must be calculated numerically.

The topological partition of the ELF gradient field [89,136] yields basins of attractors, which can be thought as corresponding to bonds and lone pairs. In a molecule one can find two types of basins, core basins and valence basins. Core basins surround nuclei with atomic number $Z > 2$ and are labeled C(A), where A is the atomic symbol of the element. Valence basins are characterized by the number of atomic valence shells to which they participate, in other words by the number of core basins with which they share a boundary. This number is called the synaptic order. Thus, there are monosynaptic, disynaptic, trisynaptic basins, and so on. Monosynaptic basins, labeled V(A), correspond to the lone pairs in the Lewis model, and polysynaptic basins correspond to the shared pairs of the Lewis model. In particular, disynaptic basins, labeled V(A, X), correspond to two-center bonds, trisynaptic basins, labeled V(A, X, Y), to three-center bonds and so on. The valence shell of a molecule is the union of its valence basins. As hydrogen nuclei are located within the valence shell, they are counted as a formal core in the synaptic order, because hydrogen atoms have a valence shell. For example, the valence basin accounting for a C—H bond is labeled V(C,H) and called protonated disynaptic. The valence shell of an atom A, in a molecule, is the union of the valence basins whose label lists contain the element symbol A.

By integrating the one-electron density over any of the core or valence basin volumes, labeled Ω_i, one obtains their average population, $\bar{N}(\Omega_i)$,

$$\bar{N}(\Omega_i) = \int_{\Omega_i} \rho(\mathbf{r})\,\mathrm{d}\mathbf{r} \tag{6}$$

When dealing with open-shell systems of particular importance are the integrated basin spin densities,

$$\langle S_z\rangle_{\Omega_i} = \frac{1}{2}\int_{\Omega_i} (\rho^{\alpha}(\boldsymbol{r}) - \rho^{\beta}(\boldsymbol{r}))\,\mathrm{d}\boldsymbol{r} \tag{7}$$

where $\rho^{\sigma}(\boldsymbol{r})$ is the σ spin one-electron density distribution function. As the basin populations are not independent ($\sum_i \bar{N}(\Omega_i) = N$), it is possible to carry out the multivariate statistical analysis of the basin populations through the definition of the covariance operator. The expectation values of this operator,

$$\langle \mathrm{cov}(\Omega_i,\Omega_j)\rangle = \int_{\Omega_i}\int_{\Omega_j} \pi(\mathbf{r}_1,\mathbf{r}_2)\,\mathrm{d}\mathbf{r}_1\,\mathrm{d}\mathbf{r}_2 - \bar{N}(\Omega_i)\bar{N}(\Omega_j) \tag{8}$$

where $\pi(\mathbf{r}_1,\mathbf{r}_2)$ denotes the spinless pair density [137], provide pieces of information on the electron delocalization. In particular, the diagonal elements, the variances $\sigma^2(\Omega_i)$, are a measure of the quantum mechanical uncertainty of the basin's population, namely the degree of *fluctuation of the electron pair*. The multivariate analysis can be used to build a phenomenological classical model of the charge distribution in terms of the superposition of weighted mesomeric structures [93]. Moreover, the covariance has a clear relationship with the so-called delocalization index (DI) $\delta(\Omega_i,\Omega_j)$, defined in the atoms-in-molecules framework by Fradera et al. [138]:

$$\langle \mathrm{cov}(\Omega_i,\Omega_j)\rangle = -\frac{\delta(\Omega_i,\Omega_j)}{2} \tag{9}$$

The DI, $\delta(\Omega_i,\Omega_j)$, accounts for the electrons delocalized or shared between basins Ω_i and Ω_j. It is worthy to note that, except for the sign, it is identical to the delocalization index we introduced in our previous studies[77,79]. As the total variance in a certain basin can be written in terms of covariance,

$$\sigma^2(\Omega_i) = \sum_{j\neq i}\langle \mathrm{cov}(\Omega_i,\Omega_j)\rangle = -\sum_{j\neq i}\frac{\delta(\Omega_i,\Omega_j)}{2} \tag{10}$$

one can do the usual contribution analysis, given usually as a percentage,

$$\mathrm{C.A.}(\Omega_i|\Omega_j) = \frac{\langle \mathrm{cov}(\Omega_i,\Omega_j)\rangle}{\sum_{i\neq j}\langle \mathrm{cov}(\Omega_i,\Omega_j)\rangle}\times 100 = \frac{\langle \mathrm{cov}(\Omega_i,\Omega_j)\rangle}{\sigma^2(\Omega_j)}\times 100 \tag{11}$$

This term thus provides us the relative contribution of the delocalized electrons of basin Ω_j on basis Ω_i.

In the context of ELF analysis, the concept of domain is very important since it enables one to define chemical units within a system and to characterize the valence domains belonging to a given chemical unit. Considering only gradient dynamical system, mathematical properties do not provide the entire set of definitions necessary to describe the bonding in molecules, and therefore some other mathematically based approaches are required for this purpose. The topological concept of domain has been introduced in chemistry by P. Mezey to recognize functional groups within organic molecules [139]. A localization domain is a region of space encompassed with an iso-ELF surface $\eta(\mathbf{r}) = f$ (a value around 0.8 is commonly chosen delimiting volumes within which the Pauli repulsion is rather weak). It is called reducible when it contains more than one attractor. Upon the increase in the value of $\eta(\mathbf{r})$, defining the bounding isosurface, a reducible domain is split into several domains, each containing fewer attractors than the parent domain. Three types of domains can be distinguished according to the nature of the attractors within them. A core domain contains the core attractor(s) of a given atom, a valence domain contains only valence attractors, and a composite domain contains both valence and core ones. For any system, there exists low values of $\eta(\mathbf{r}) = f$ defining a unique composite parent domain. The successive reductions of localization will split this parent domain. Every child which is a composite domain corresponds to one or more chemical species. A chemical unit is the union of the basins of the last appearing composite domain of a branch provided; it is a filled volume. The reduction of localization occurs at turning points, which are critical points of index 1 located on the separatrix of two basins involved in the parent domain. Ordering these turning points (localization nodes) by increasing $\eta(\mathbf{r})$ enables to build tree-diagrams reflecting the hierarchy of the basins. For example, it allows to build-up a scale for the weak and medium hydrogen bond, by defining a core valence bifurcation (CVB) index, introduced by Fuster and Silvi [96] and applied recently by Alikhani et al. [116]. This index is positive when the first bifurcation creates two molecular reducible domains (for weak H-bonded complexes) and negative when the core-valence separation is the first bifurcation occurring in the reduction of the localization process (for medium H-bond complexes which can thus be considered as single molecules).

APPLICATION TO TWO-CENTER THREE-ELECTRON BONDS

Computational Methods

The calculations were performed with the Gaussian94 [140] (for the H_nXYH_m-type systems), the Gaussian98 [141] (for the SO radicals), and the Gaussian03 [142] (for the textbooks examples) computational chemistry packages. At the present state of the art, the topological analysis of the ELF gradient field requires a wavefunction expressed in terms of a single determinant, built on Hartree–Fock or Kohn–Sham orbitals (work is in progress to perform the analysis on correlated wavefunctions). For the textbook examples, different methods of calculations, ROHF, ROB3LYP, and ROBH&HLYP (where RO stands for spin-restricted open-shell formalism), were tested to study their influence on the ELF results. For the H_nXYH_m molecules and their anionic radicals, the optimizations of the geometries, as well as the calculations of the wavefunctions, were carried out with the hybrid density BH&HLYP functional [87], within the spin-unrestricted formalism, in the standard 6-311++G(3*df*, 2*p*) basis set. For the unsubstituted SO radicals, the structures were optimized at the coupled-cluster level with inclusion of single and double excitations and perturbative treatment of the triple excitations [CCSD(T)] in the 6-31+G* basis set and a single energy point was calculated with the BH&HLYP functional. For the substituted molecules, full optimization was performed at the MP2/6-31+G* level, followed by a partial optimization at the CCSD(T)/6-31+G*, and finally a single-point energy calculation with BH&HLYP/6-31+G*. The evaluation of the ELF function on a grid, as well as the various steps of the topological analysis described above, was carried out with the TopMoD program [143,144], developed in our laboratory and visualized with the molekel 4.3 software [145].

Textbook Examples

Three types of calculations (ROHF, ROB3LYP, and ROBH&HLYP) were applied to prototype 2c-3e bonded systems, namely the rare gas dimer cation radicals He_2^+ (first example given by Pauling in his book [2]) and Ne_2^+. The bond distances and dissociation energies obtained with these three methods, using the 6-311+G(3df,2p) basis set, are reported in Table 1 and compared with experimental values. As already discussed by Hiberty et al. [56], HF generates poor dissociation energies that always

TABLE 1 Equilibrium Distances (R_e), in angströms (Å) and Dissociation Energies (D_e), in kcal.mol^{-1}, of He_2^+ and Ne_2^+ Obtained with Different Methods of Calculation and by Using the 6-311+G(3df,2p) Basis Set

	He_2^+		Ne_2^+	
Method	R_e	D_e	R_e	D_e
ROHF	1.0604	38.1	1.6897	−2.9
ROB3LYP	1.1425	75.5	1.8373	59.2
ROBH&HLYP	1.0993	65.5	1.7522	37.8
Exp	1.081[a]	56.9[a]	1.75[a]	31.4[b]

[a]From Huber and Herzberg [153].
[b]From Dehmer and Pratt [154].

largely underestimate the experimental results (and are even negative in the case of Ne_2^+). Nevertheless, the HF bond distances are in good agreement with the experiment. On the contrary, the B3LYP method provides overestimated bond energies and, in apparent contradiction, bond lengths that are too large. These errors have already been observed by Braïda et al. [58] whatever the functional used (local spin density, gradient corrected, or hybrid functional) and have been interpreted "as consequences of electron self-interaction, leading to overstabilization of the Coulombic terms relative to the exchange–correlation terms." Finally, the BH&HLYP functional performs surprisingly well, as also initially pointed out by Braïda et al. [58], especially in what concerns bond distances. In spite of the heterogeneousness of these structural and energetical results, the topological descriptors are very homogeneous, which is crucial when considering the aim of this paper. First, on a qualitative point of view, the ELF-based topology of the two cation dimers X_2^+ is the same, i.e., it is composed of two core basins C(X) and two monosynaptic basins V(X), one for each X atom, and there is *no* disynaptic basin V(X,X) between the two nuclei. Second, the topological descriptors of these complexes, i.e., the population, integrated spin density, and variance of the V(X) basin, reported in Table 2, do not depend either on the method of calculation employed. Focusing on He_2^+, the population and integrated spin density of the V(He) basins show that the unpaired electron is equally shared between both atoms. Moreover, there is a large covariance matrix element between the two monosynaptic basins, which is the ELF signature of an important electron fluctuation between the two lone pairs. Hence, there is a perfect agreement between the ELF-based description and the Pauling resonance scheme of the 2c-3e bond below,

$$\mathrm{He}\!:\cdot\mathrm{He}^+\,(50\%) \leftrightarrow \mathrm{He}^+\!\cdot\!:\mathrm{He}\,(50\%)$$

For Ne_2^+, the deviation of the V(Ne) population and spin density from "Lewis" values (7.5 *e* and 0.25, respectively) is due to the small contribution of the Ne cores to the resonance process.

TABLE 2 Topological Descriptors of Model Systems, Using Three Different Methods of Calculations: Population $\bar{N}$, Integrated Spin Density $\langle S_z \rangle$, and Variance σ^2 of the Monosynaptic Basin

System	*Method*	$\bar{N}$	$\langle S_z \rangle$	σ^2
He_2^+	ROHF	1.50	0.25	0.31
	ROB3LYP	1.50	0.25	0.30
	ROBH&HLYP	1.50	0.25	0.31
Ne_2^+	ROHF	7.32	0.24	0.71
	ROB3LYP	7.44	0.24	0.70
	ROBH&HLYP	7.38	0.24	0.71

Among the other systems that have been proposed by Pauling as candidates for 2c-3e bonding molecules, we have chosen to investigate the three following: nitric oxide, the most stable of the odd-electron molecule, oxygen monofluoride, and chlorine dioxide. Our aim is to verify whether Pauling's predictions are supported by the ELF analysis. The equilibrium bond lengths and angles, calculated in the framework of the BH&HLYP functional, are reported in Table 3 and are compared with experimental or other theoretical results. The agreement is reasonable for NO and ClO_2 and very good for FO. The ELF-based topology of these three molecules differs from the one of the rare gas dimer cations, since they are not purely 2c-3e bonded compounds. Indeed, disynaptic V(X,O) basins (X = N, F, Cl) reveal the shared-electron pair character of the X–O bonds in the three radicals. More insights in the nature of these bonds are provided by the quantitative topological descriptors, i.e., the basin populations, their variance, and the basin integrated spin densities, which are reported in Table 4.

For the NO molecule, the $\langle S_z \rangle$ values indicate that the V(N) basin contributes 60% to the localization of the unpaired electron, whereas the V(O) basin

TABLE 3 Bond Lengths R_e, in Å, and Bond Angles α, in degrees, of Three Neutral Radicals Proposed by Pauling As Candidates for 2c-3e Bonded Molecules

Molecule	R_e	α
NO	1.1268	
	1.1577[a]	
FO	1.3204	
	1.32[b]	
ClO_2	1.4455	116.6
	1.470[c]	117.4033[c]

First line: ROBH&HLYP/6-311+G(3df,2p) optimized values. Second line: experimental or other theoretical values.
[a]From Horn and Dickey [155].
[b]From O'Hare and Wahl [156].
[c]From Kuchitsu [157].

TABLE 4 Topological Descriptors of Model Systems: Valence Basins Population $\bar{N}$, Basin Integrated Spin Densities $\langle S_z \rangle$, and Variance of the Basin Populations σ^2

Molecule	*Basin*	$\bar{N}$	$\langle S_z \rangle$	σ^2
NO	V(N)	3.7	0.30	0.86
		3.7	*0.33*	*0.57*
	V(N,O)	2.4	0.02	1.14
		2.5	*0.00*	*0.73*
	V(O)	4.7	0.15	1.12
		4.8	*0.16*	*0.64*
FO	V(F)	6.7	0.06	0.72
	V(F,O)	0.6	0.00	0.44
	V(O)	5.5	0.40	0.64
ClO_2	V(Cl)	4.1	0.20	1.16
		4.4	*0.20*	*0.24*
	V(Cl,O)	1.4	0.00	0.81
		1.5	*0.00*	*0.80*
	V(O)	5.7	0.13	1.04
		5.9	*0.14*	*0.28*

The values in roman characters have been obtained from an ELF calculation using a ROBH&HLYP/6-311+G(3df,2p) wavefunction, those in italics, result of a phenomenological model in terms of Lewis resonance structures (see text).

contributes 30%. When the core basins are taken into account, the contribution of the nitrogen atom amounts 64%, whereas the contribution of the oxygen atom only 32%. At first the resonant scheme of Pauling (see Fig. 2) seems in agreement with our ELF analysis. Moreover, the large covariance between the two monosynaptic basins (−0.42) supports this analysis. However, the value of the V(N,O) population is closer to 2 than to 4, therefore the N—O bond is a single bond rather than a double one. Hence, the resonance scheme for the NO radical should contain at least one structure with a single N—O bond. Figure 3 displays the four Lewis structures that we propose to describe the NO radical in the framework of this phenomenological model. The weights of each structure have been determined such as to best reproduce basin populations and integrated spin densities. Indeed these "phenomenological" ELF descriptors, reported in Table 4, compare well with the theoretical values. The covariance matrix elements have been recalculated a posteriori, and the agreement is not so good (all the values are systematically found too small). Only the diagonal values, i.e., the variances on the basin population, are reported in Table 4. The results could be improved by adding other ionic and no-bond structures, but the fundamental features of the bonding are already contained in the model (Fig. 3). Our phenomenological model suggests that the the N—O molecule can be described by the following interactions in resonance:

1. a three-electron bond superimposed to a single bond, represented by the resonance between structures I and II,
2. a double bond represented by structure III, where the lone electron is localized on N, and
3. a simple bond with partial charges, where the lone electron localized on N, represented by structure IV.

For the OF radical, the resonance scheme of Pauling, reported in Fig. 4, would imply that the unpaired electron is shared between the two atoms. However, the ELF results do not at all support this description, as the integrated spin density of the V(F) basin is very small. Indeed, when the core basins are taken into account, one finds that the oxygen atom contributes 90% to the localization of the lone electron. As a result, this precludes the existence of a three-electron bond in the molecule. The very low population of the V(F,O) (0.6 *e*), as well as the large correlation between the V(O) and V(F) monosynaptic basins, is in favor of a charge-shift electron-pair (CS) scheme of the bonding, involving ionic structures such as F^+O^- and F^-O^+, as in F_2. In this type of bonding, recently revisited by Shaik et al. [146], the two atoms are held by the exchange of two lone pairs rather than by the exchange of a lone pair and of an electron, which characterizes the 2c-3e bond.

For ClO_2, the integrated spin density of the V(Cl) basin is of the same order of magnitude as that of each V(O) basin (0.20 vs. 0.13). The covariances between the V(Cl) and each V(O) basin are large (−0.36), which indicates that the electron fluctuation between the two centers is an important phenomenon. However, the population of the V(Cl,O) disynaptic basins is smaller than 2. The resonance scheme proposed by Pauling (see Fig. 5) is therefore incomplete and no-bond or ionic structures must be taken into account. We thus propose the resonance scheme in Fig. 6. It is noteworthy that the figure displays only half of the Lewis structures; the three missing ones I′, II′, and III′ are obtained by exchanging the roles of the two equivalent oxygen atoms. The population obtained from this phenomenological model (see Table 4) are in good agreement with those calculated within the ELF analysis; concerning the electron fluctuation only the variance of the V(Cl,O) basin is well reproduced. Nevertheless, if we adopt this model, the bonding in ClO_2 can be described in the following way:

1. The main contribution arises from the resonances between symmetric structures I and I′, II and II′, because of the electron delocalization between the two equivalent oxygen atoms. Ionic structures III and III′ are only minor contributions.
2. Structure I (respectively I′) resonates with structure II (respectively II′) by electron transfer from

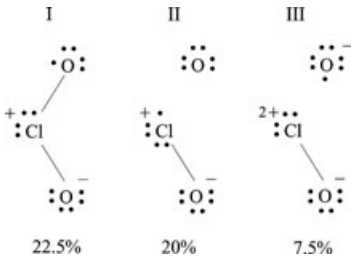

FIGURE 6 The Lewis resonant structures inferred from the ELF description of ClO_2. The complete resonant scheme involves three other similar structures (I′, II′, and III′), taking into account the electron delocalization between the two equivalent oxygen atoms.

the "up" oxygen atom (respectively "down" O) to the chlorine atom but, on the contrary to the 2c-3e bonding scheme proposed by Pauling, there is no electron pair transfer from Cl to the "up" O (respectively "down" O), and consequently no global charge transfer. Charge conservation is ensured by the relocalization of the bonding Cl—O pair on the oxygen atom.

The $H_nX\therefore YH_m^-$ Anion Radicals

In the original paper, we investigated the formation of a two-center three-electron bond by attachment of an electron on a molecule of the H_nXYH_m type (with X,Y from the second and third lines of the periodic table and n, m taking the appropriate values between 0 and 3) [77]. As we were particularly interested by the topological changes occurring during this process, we first considered the vertical attachment (by conservation of geometry) and then removed this constraint by relaxation. Here, we focus on molecules isoelectronic to Cl_2 (i.e., X,Y = Cl, S, P, Si and n, m = 0–3) as a representative set of this type of compounds. We reinterpret the vertical processes in a simpler manner and we rediscuss the nature of the X—Y bond of some compounds.

Structural Description of the Electron Attachment Process. The geometry of the H_nXYH_m systems and their associated radical anions were fully optimized. The structures of the compounds with X, Y = Cl, S, P, Si, depicted in Fig. 7, together with pertinent geometrical data, are consistent with expectations based on standard bond lengths and bond angles. Going from X = P to X = Si, however, the X—Y bond length increases less than expected and even decreases slightly from H_2PCl to H_3SiCl, illustrating the particular nature of the Si atom. When an electron is attached to the system, the most dramatic effect on the geometry is the lengthening of the bond distance, by an amount of 0.66 Å for Cl_2^- (i.e., an

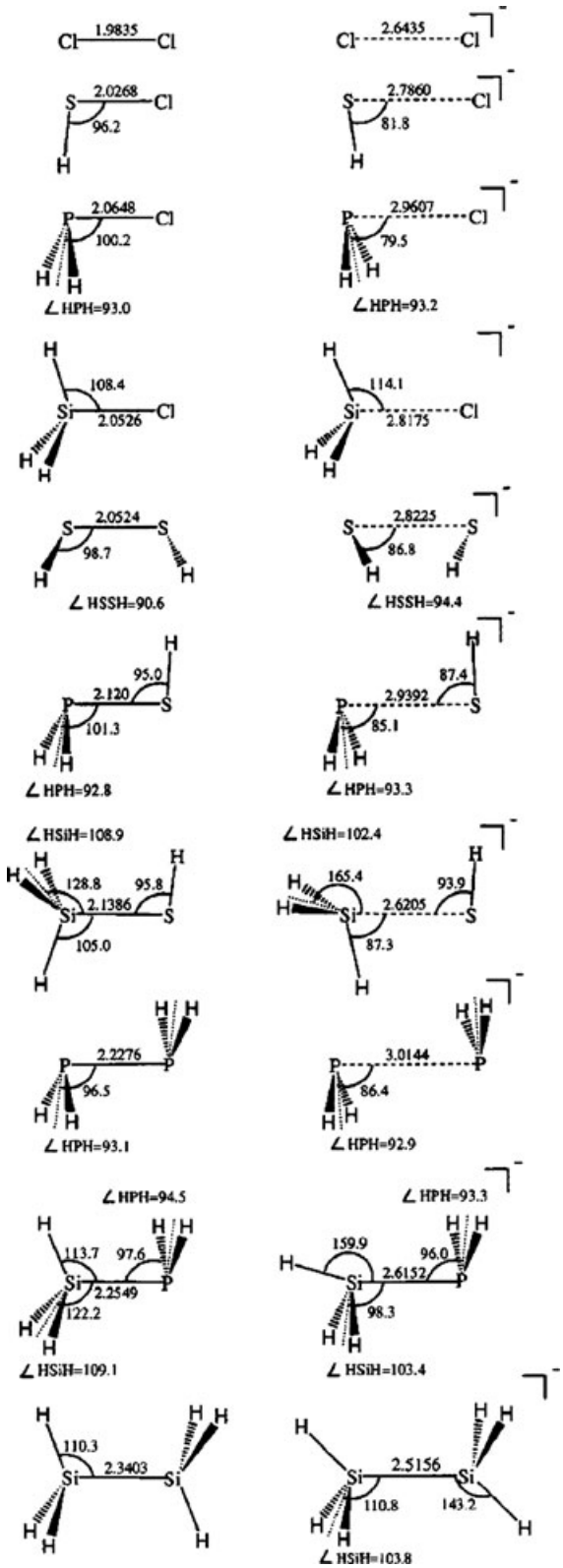

FIGURE 7 BH&HLYP-optimized structures for H_nXYH_m systems (left-hand side) and their associated radical anions (right-hand side), with X, Y = Cl, S, P, Si and n, m = 0, 1, 2. The 6-311++G(3*df*,2*p*) basis set was used for all the systems. Distances are in angstroms and angles are in degrees.

increase of ~30%), 0.90 Å for H_2PCl^- (i.e., an increase of ~43%) but only 0.175 Å for $H_6Si_2^-$(7%). This is consistent with the decrease of the formal bond order from 1 to 0.5, arising from the description of the process in terms of MO theory. For a given Y atom, the X–Y distance increases as X changes from X to P and *decreases* from P to Si, which denotes the special behavior of the compounds containing Si. Moreover, one observes a decrease of the ∠HXY and ∠HYX angles, except again for X or Y = Si. Indeed, the geometry of the Si-containing anionic compounds is very particular, not only because of the slight increase in the Si—Y bond lengths but also because of the change of orientation of the SiH_3 moiety, in such a way that its HOMO points to a direction that is largely deviated from the Si–Y axis. This lets us to postulate that these anions may exhibit a bonding scheme that is more complex than a simple three-electron bond, as already pointed out by Braïda et al. for $H_6Si_2^-$ [75].

The dissociation energy D_e obtained with BH&HLYP for the neutral compounds and the associated anions are reported in Table 5. Consistent with the lengthening of the X—Y bond, one observes a decrease of D_e upon electron attachment, which ranges from 8.5 kcal mol^{-1} for H_2PCl^{-1} to 30.7 kcal mol^{-1} for Cl_2 (typical values for 2c-3e bonding energies are of the order of 20–30 kcal mol^{-1}). For homonuclear compounds, the bonding energies are found to decrease for heavy atoms across the periodic table from right to left, as already pointed out by Braïda et al. in their study of stability of three-electron bonded radical anions [75]. Moreover, in a series of anions as H_nXCl^-, with (X,*n*) = (Cl,0), (S,1), (P,2), and (Si,3), the variation of D_e (decreasing from X = Cl to P and then increasing from P to Si), is in agreement with that of R_e, as for the bond distance. Finally, our results compare well with other theoretical calculations and experimental data, where such data are available.

TABLE 5 Dissociation Energy (kcal mol^{-1}) for the H_nXYH_m Molecules Isoelectronic to Cl_2 and for the Associated Radical Anions, Calculated at the BH&HLP/6_311++G(3df,2p) level. (see text)

Species	*Symmetry*[a]	*This work*	*From Literature*	*Experimental*
Cl_2	$D_{\infty h}$	49.8		57.3[b]
Cl_2^-	$D_{\infty h}$	30.7	28.10[c]	31.8[d]
HSCl	C_s	58.9		
$HSCl^-$		15.3		
H_2PCl	C_s	76.0		
H_2PCl^-		8.5		
H_3SiCl	C_{3v}	104.8		
H_3SiCl^-		10.3		
H_2S_2	C_2	59.8	58.22[e]	
$H_2S_2^-$		26.0	25.74[f]	
H_2PSH	C_s	64.5		
H_2PSH^-		13.5		
H_3SiSH	C_s	87.7		
H_3SiSH^-		18.0		
H_4P_2	C_{2h}	55.8	53.36[e]	
$H_4P_2^-$		21.0	21.43[f]	
H_3SiPH_2	C_s	71.2		
$H_3SiPH_2^-$		27.2		
H_6Si_2	D_{3d}	74.1	73.49[e]	
$H_6Si_2^-$	C_{2h}	28.7	30.19[f]	

[a]Otherwise specified, the neutral compound and its anion have the same symmetry.
[b]From Huber and Herzberg [153].
[c]From Braïda and Hiberty [50].
[d]From Dojhan and Chen [49].
[e]CASPT2/ccpVTZ [75].
[f] CCSD(T)/aug-ccpVTZ [75].

ELF-Based Topological Description

Analysis of the Electron Attachment Process. Figure 8 depicts the ELF = 0.8 localization domains of the symmetrical $H_{2n}X_2$ species (with (X,*n*) = (Cl,0), (S,1), (P,2)), of the associated vertical radical anions, and of the 3e-bonded radical anions. They typify, from a topological point of view, three different mechanisms of 3e bond formation.

Neutral Molecules: The topology of the $H_{2n}X_2$ neutral molecules (see panels (a) of Fig. 8) are composed of (i) two core basins C(X) and C(X′); (ii) 2*n* protonated disynaptic basins V(X,H), each associated with the electronic pair of a X—H bond; (iii) from the Lewis representation of these molecules, we expect $6 - 2n$ monosynaptic basins V(X), each related to a lone electron pair. This rule is valid for H_4P_2 and H_2S_2, but in Cl_2 the lone pairs of each atom are gathered in a single basin V(Cl) by the cylindrical symmetry; (iv) one disynaptic V(X,X′) basin, which is the usual signature of a covalent bond. The populations of the valence basins, reported in Table 7, are consistent with expectations based on the electronegativity of the central atoms of the compounds. For instance, the V(X,X) population of the homodimeric H_nXXH_n molecules is found to decrease with X across the periodic table from left right, from1.8 *e* for H_4P_2 to 1.0 *e* for Cl_2, which illustrates the increase of the ionic contribution of the X—X bond. Concomitantly, the excess of population of the V(X) basins with respect to a standard Lewis structure increases from X = P to X = Cl. For heterodimeric species with Y constant, say Y = Cl, the population of the V(X,Y) basin increases as X varies from Cl to Si, as expected from the increase in the difference in electronegativity between the two heavy atoms.

Before investigating the effect of electron attachment, it is worthy to note that the concept a

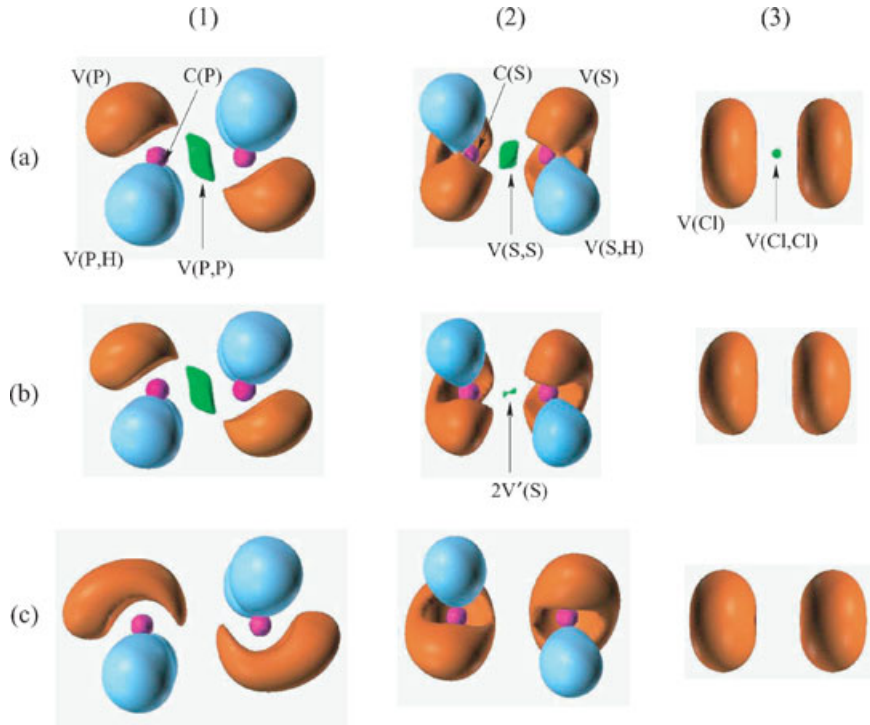

FIGURE 8 ELF = 0.8 isosurfaces for the H_nX_{2n} compounds, (a), and their associated vertical, (b), and relaxed, (c), radical anions; (1) H_2S_2, (2) H_4P_2, and (3) Cl_2.

electron-pair bonding has recently been revisited by Shaik et al. in the framework of both VB theory and ELF approach: "both types of calculations point to the conclusion that, along the two classical bond families of covalent and ionic bonds, there exists a distinct class of charge-shift bond (CS-bonds) in which the fluctuation of the electron-pair density plays a dominant role" [146]. These bonds are characterized in VB theory by a large covalent–ionic resonance energy and in ELF by a depleted basin population (smaller than 2.0 *e*), a large variance, and negative covariance. The Cl_2 molecule is a prototype (with F_2) for CS-bonded molecules, with a small population of 1.0 *e*, a variance of 0.74, and a covariance of −0.7. Atoms (or fragments) that are prone to CS bonding are compact electronegative and/or lone-pair-rich species, albeit with moderate electronegativity. The HSCl, H_2PCl, H_3SiCl, H_2S_2, H_2PSH, and H_4P_2 compounds can also be classified into this family, in which "the bonding arises rather from the covalent–ionic fluctuation of the electron pair density" [146].

Vertical Anions: If we restrict ourselves to the topological changes arising *around the bonding region*, we can distinguish three different behaviors upon vertical attachment. These are classified as a function of the value of the morphic number, $\Delta\mu_v$, which is the variation of the number of basins in the valence region.

1. $\Delta\mu_v = 0$: The number and type of basins remain identical as in the neutral molecule. H_4P_2 is a representative member of this set, which is also made up of all the compounds containing the Si atom, as well as H_2PCl and H_2PSH. Here, the electron attachment is a process in which the molecule stays in the same domain of structural stability. In the context of catastrophe theory, such a process is called a tautomorphic one.
2. $\Delta\mu_v = 1$: The number of basins increases by one, because of the splitting of the V(X,Y) basin into two monosynaptic basins V′(X) and V′(Y), as in H_2S_2. Such a process is called a polymorphic process. The newly created basins, each centered on the axis linking the two heavy atoms cores, characterize a protocovalent bond in the vertical state. The only other member of this set is HSCl.
3. $\Delta\mu_v = -1$: The number of basins decreases by one, because of the disappearance of the V(X,Y) basin, as in Cl_2. This is a miomorphic process.

The latter classification corresponds more or less to three domains of variation of the vertical electron affinity (vEA) of the compounds, which are

TABLE 6 BH&HLYP/6-311++G*(3df,2p)* Calculations (in kcal mol^{-1}) for the H_nXYH_m Molecules

Species	*vEA*[a]	*aEA*[b]
Cl_2	16.8	61.1
HSCl	−2.1	37.8
H_2PCl	−14.5	14.8
H_3SiCl	−24.1	−15.6
H_2S_2	−15.7	15.4
H_2PSH	−18.7	−0.9
H_3SiSH	−19.5	−18.7
H_4P_2	−17.6	−10.3
H_3SiPH_2	−19.1	−19.1
H_6Si_2	−22.1	−19.4

[a]Vertical electron affinity (i.e., using the energy of the vertical anion).
[b]Adiabatic electron affinity (conventional electron affinity).

reported in Table 6. Indeed the vEA of the molecules of the "H_4P_2 set" are all negative and very low, around −20 kcal mol^{-1} except for H_2PCl, so that the vertical anions are not stable. The vEA value of H_2S_2 and HSCl is still negative but greater. Cl_2 is the only system with a positive vEA, which means that the vertical anion is more stable than the neutral, because of the large electronegativity of the Cl atom. Examination of the integrated properties in Table 7 allows us to determine where the extra electron is located according to the preceding classification.

1. Let us consider the H_4P_2 molecule, as a representative member of this set. We note that only half of the extra electron density is located in the valence basins: the monosynaptic ones only absorb 0.1 *e* each and the disynaptic protonated ones around 0.07 *e* each (it has been observed that the maximum population of a V(P,H) basin is around 2.2 *e*), whereas the population of the disynaptic V(P,P) basin remains unchanged. The remaining 0.5 *e* is distributed among four newly created asynaptic basins ($\Delta\mu = +4$). The attractors of these basins are located far from the bonding region, beyond the V(P,H) basins, and their ELF value is lower than 0.8 (actually around 0.5) which explains why the corresponding domains are not seen on Fig. 8. The associated electron density is thus described to a great extent by Rydberg orbitals, and is therefore not really captured by the molecule. Similar trends are observed for all the members on this set, in particular the total population of the asynaptic basins is always greater or equal than 0.5 *e*. The basin integrated spin densities, also reported in Table 7, confirm the nearly equal sharing of the extra electron density between the valence (monosynaptic plus protonated) and asynaptic basins (the sum of the spin density is not exactly equal to 0.5, because the small contributions of the core are not indicated). The contribution of the asynaptic basins increases more or less as the vEA decreases (except for the vertical anion H_3SiCl^-), up to reach a population of 0.7 *e* and an integrated spin density of 0.31 in the vertical anion $H_6Si_2^-$.
2. For H_2S_2, the splitting of the V(X,Y) basin into two monosynaptic basins is accompanied by a lowering of the associated population, from 1.5 to 2×0.5 *e*. In contrast with the compounds of the H_4P_2 type, there is now a subsequent transfer of electron density toward the V(S) basins ($2 \times 0.4\,e$), whereas each V(H,S) basin absorbs 0.06 *e*. We still observe the creation of asynaptic basins beyond the protonated disynaptic basins, but the population is smaller in the previous group, 0.4 *e*, since the molecule is a better electron acceptor. Observation of the integrated spin density clearly shows the enhancement of the localization of the unpaired electron into the lone pairs of each sulfur atom, whose total contribution to $\langle S_z \rangle$ becomes now dominant (44%) with respect to the asynaptic basins (34%). These trends are substantially accentuated in HSCl, for example, 40% of the spin is now located into the V(S) basin, 32% into the V(Cl) basin, whereas the asynaptic basins contribute to no more than 10%.
3. In Cl_2, which has a positive vEA (and as a consequence, a positive aEA), the vertical attachment results in the disappearance of the disynaptic V(Cl,Cl′) basin and no asynaptic basin is created. Because of the large electronegativity of the molecule, the monosynaptic basins are able to absorb the V(Cl,Cl′) population plus the extra electron, i.e., 1.0 *e* each. The $\langle S_z \rangle$ value shows that the extra unpaired electron is equally shared by the two chlorine lone pairs. As will be seen shortly, the vertical anion Cl_2^- presents the typical topology of the relaxed 2c-3e anions.

Relaxed anions: The geometry relaxation, corresponding mainly to a lengthening of the X—Y bond, makes disappear either the disynaptic V(X,Y) basin (as in $H_4P_2^-$) or the monosynaptic V′(X) and V′(Y) basins arising from the splitting of the V(X,Y) one (as in $H_2S_2^-$), as well as all the asynaptic basins appeared during the vertical attachment (except for Cl_2^- in which the vertical anion already presents a "3e-type" ELF topology). For X = Y, the topology of the 3e-bonded radical anions (Fig. 8c) is thus composed by (i) two core basins C(X), (ii) 2*n*-protonated V(X,H) basins, and (iii) $6 - 2n$ monosynaptic basins V(X) (2 for Cl_2^-) such that the net variation of the number of basins with respect to the neutral state is $\Delta\mu = -1$. In the framework of the catastrophe theory, such a process with $\Delta\mu < 0$ is called

TABLE 7 ELF-Based Topological Properties for the H_nXYH_m Molecules (X,Y = Cl, S, P, Si; n, m = 0–3)

	$V(X,Y)$	$V(X)$		$U[V(X,H_i)]_{i=1,n}$		$V(Y)$		$U[V(Y,H_i)]_{i=1,m}$		$U Asyn$				
H_nXYH_m	$\bar{N}$	$\bar{N}$	$\langle S_z \rangle$	$\bar{N}$	$\langle S_z \rangle$	$\bar{N}$	$\langle S_z \rangle$	$\bar{N}$	$\langle S_z \rangle$	$\bar{N}$	$\langle S_z \rangle$	$\Delta\mu_v$	$\Delta\mu$	δ(V(X), V(Y))
Cl_2	1.0	6.4				6.4								0.70
va		7.4	0.23			7.4	0.23					−1	−1	1.14
a		7.4	0.23			7.4	0.23					−1	−1	0.70
HSCl	1.2	4.3		1.89		6.5								0.48
va	0.6[a]	5.0	0.20	1.96	0.03	7.1	0.16			0.1	0.05	+1	+2	0.98
a		5.3	0.30	1.92	0.03	7.6	0.14					−1	−1	0.51
H_2PCl	1.4	2.0		4.00		6.5								0.18
va	1.1	2.3	0.08	4.14	0.07	6.9	0.09			0.5	0.20	0	+1	0.25
a		3.0	0.30	4.10	0.09	7.8	0.08					−1	−1	0.09
H_3SiCl	1.5			5.97		6.4								
va	1.5			6.18	0.11	6.6	0.08			0.5	0.22	0	+1	
a		0.9	0.17	6.22	0.20	7.8	0.10					0	0	0.19
H_2S_2	1.5	4.3		1.91		4.3		1.91						0.40
va	1.0[b]	4.7	0.11	1.97	0.03	4.7	0.11	1.97	0.03	0.4	0.17	+1	+3	0.95
a		5.5	0.21	1.91	0.02	5.5	0.21	1.91	0.02			−1	−1	0.54
H_2PSH	1.6	2.0		4.00		4.3		1.88						0.16
va	1.6	2.1	0.06	4.10	0.06	4.4	0.05	1.91	0.02	0.5	0.23	0	+3	0.98
a		3.1	0.25	4.10	0.07	5.7	0.14	1.92	0.01			−1	−1	0.39
H_3SiSH	1.8			5.96		4.2		1.88						
va	1.8			6.13	0.08	4.3	0.06	1.92	0.04	0.6	0.29	0	+2	
a		1.2	0.18	6.08	0.14	5.6	0.13	1.95	0.01			0	0	0.46
H_4P_2	1.8	2.1		3.96		2.1		3.96						0.10
va	1.8	2.2	0.04	4.08	0.06	2.2	0.04	4.08	0.06	0.5	0.22	0	+4	0.11
a		3.4	0.19	4.06	0.04	3.4	0.19	4.06	0.04			−1	−1	0.39
H_2PSiH_3	1.9	2.0		3.96				5.98						
va	1.9	2.2	0.06	4.02	0.05			6.15	0.09	0.6	0.26	0	+2	
a	1.2	2.4	0.12	4.04	0.03	1.2	0.17	6.03	0.11			+1	+1	0.13
H_6Si_2	1.9			5.95				5.95						
va	1.9			6.07	0.06			6.07	0.06	0.7	0.31	0	+6	
a	1.0[b]	0.9	0.13	6.05	0.10	0.9	0.13	6.05	0.10			+3	+3	0.10

Valence basin populations, $\bar{N}$, for the neutral ground state, the vertical anion (va), and the relaxed anion (a). Basin integrated spin densities, ($\langle S_z \rangle$) for the open-shell anionic compounds (always negligible for the V(X,Y) basins, i.e., < 0.01). To simplify the discussion, the monosynaptic basins of each given center have been merged.
The U symbol means that we have performed the sum of the integrated properties over the indicated basins.
$\Delta\mu_v$ (respectively $\Delta\mu$) is the variation of the number of basins in the valence region (respectively in the whole space) with respect to the neutral molecule.
δ(V(X), V(Y)) is the index of delocalization (see text).
[a]Sum of the populations of the V′(S) (0.2 *e*) and V′(Cl) (0.4) monosynaptic basins.
[b]Sum of the (equal) populations of the two $V_1(X)$ and $V_2(X)$ basins.

miomorphic. For $X \neq Y$, the 3e bond formation also corresponds to a *miomorphic* process, except when one of the heavy atoms is a saturated atom (here Si, see Table 7), where the number of basins in the anion is the same as in the neutral ($\Delta\mu = 0$, *tautomorphic* process): indeed, the disappearance of the disynaptic basin is accompanied by the creation of a V(Si) basin, which was inexistent in the neutral state. Finally, the only radical anions not obeying the $\Delta\mu = -1$ or $\Delta\mu = 0$ rule are $H_2PSiH_3^-$ ($\Delta\mu = +1$) and $H_6Si_2^-$ ($\Delta\mu = +3$). In the former, the presence of a disynaptic V(P,Si) basin indicates keeping of the shared-electron pair character of the bond in the anion, whereas in the latter two monosynaptic V′(Si) between the two Si cores are the signature of the protocovalent character of the bond. For these compounds, it is worthy to note that the variation of the X—Y bond length is smaller than for the other isoelectronic to Cl_2^- radical anions. On a quantitative point of view (Table 7), the disappearance of the disynaptic and asynaptic basins results in the transfer of their population toward the monosynaptic basins (the variation of the protonated ones being comparatively very low). In $H_{2n}X_2^-$ compounds, the charge in the monosynaptic basin (5.5 *e* vs. 5 *e* for H_2S_2) used in conjunction with the integrated spin density $\langle S_z \rangle$ (0.21 in $H_2S_2^-$) shows that the additional electron is (i) uniformly distributed between both subsystems and (ii) mainly localized into the monosynaptic basins. More precisely, the spin density of the whole H_nX fragment remains constant (0.23), but each added V(X,H) basin carries away a small contribution of 0.02. It is noteworthy that the decrease of the V(X) contribution, $Cl_2^-(0.23) \rightarrow H_2S_2^-(0.21) \rightarrow H_4P_2^-(0.19)$, is then nearly proportional to the decrease of the 3e-bond energy ($30.7 \rightarrow 26.0 \rightarrow 21.0$ kcal mol^{-1}). For 3e-bonded radical anions with $X \neq Y$, the most electronegative atom tends to close its valence shell, as illustrated by the variation of the V(Cl) population and integrated spin density along the series $Cl_2^- \rightarrow HSCl^- \rightarrow H_2PCl^-$: $7.4e/0.23 \rightarrow 7.6e/0.14 \rightarrow 7.8/0.08$. This localization of the lone electron into the monosynaptic basins should be corrected when one of the heavy atom is a saturated atom, as Si: indeed, the (dominant) part of the integrated spin density borne by the XH_3 fragment is spread over the V(X) and the three V(X,H) basins, which therefore play the role of a lone-pair basin. At this stage, it is noteworthy that the weights of the resonant Lewis structures can be estimated from the $\langle S_z \rangle$ value. For example, in the case of HSCl, if one includes the small V(H,S) contribution into the dominant V(S) ones, one finds

$$H\dot{S}\ \ddot{\dot{C}}l^- \ (\sim 70\%) \longleftrightarrow H\ddot{\dot{S}}^-\ \dot{C}l (\sim 30\%)$$

thereby establishing a quantitative correspondence between the VB and topological descriptions of the 3e bond.

Analysis of the Electron Delocalization. Up to now, we have discussed the topological changes arising upon electron attachment in a molecule and have obtained useful information on the *localization* of the extra electron density in 3e-bonded radical anions. However, as stressed by Hiberty et al. [57], "the three-electron bond is nothing but a pure fluctuation of an electronic charge from one fragment to another." Unfortunately, the MO or VB descriptions of such bonds do not provide any direct measure of this fluctuation. One a posteriori verifies, considering some structural properties as equilibrium geometry or dissociation energy or through the value of the VB resonance energy that this phenomenon is correctly taken into account. In contrast, starting from a given quantum mechanical calculation of the molecule, the topological analysis of the ELF gradient field allows, as described in the section "A Sketch of the ELF Analysis," to characterize directly and quantitatively the electron *delocalization* for each molecular basin. Since the formation of a $X\therefore Y^-$ bond upon electron attachment is accompanied by a transfer of electron density toward the lone-pair basins V(X) and V(Y), one is induced to think that the electron fluctuation responsible for the stability of the 3e bond takes place principally between these basins. Therefore, correct ELF-based descriptors are related to the covariance matrix, more precisely, to the delocalization index δ(V(X),V(Y)). This index is reported in Table 7, together with the values calculated for the neutral molecules and their vertical anions.

Let us first focus on a single compound, say Cl_2, and compare the values obtained for the neutral molecule, its vertical anion, and the relaxed 3e-bonded radical anion. The large increase of δ(V(Cl),V(Cl)) upon vertical electron attachment is related to the disappearance of the disynaptic basin and to the transfer of the corresponding electron density toward the monosynaptic basins. Upon geometry relaxation, one may be surprised that δ(V(Cl),V(Cl)) has the same value as in the neutral compound. The contribution analysis of the variance of one of the monosynaptic basins, say V(Cl_1), allows understanding of this apparently paradoxical evolution as shown in Table 8 [147]. From the neutral to the vertical anion, this contribution increases from 30% to 50%, because of the complete transfer of the V(Cl_1,Cl_2) population to the lone pair. Upon relaxation, this contribution decreases to 38%, because of the lengthening of the bond

TABLE 8 Population of the Monosynaptic $V(X_1)$ Basin, $\bar{N}$, Standard Deviation, $\sigma(\bar{N})$ and Contribution of Other Basins (%) to σ^2 ($\bar{N}$) for the $H_{2n}X_2$ Molecules and $H_{2n}X_2^-$ Radical Anions (va = Vertical Anion, a = Relaxed 3-Electron Bonded Anion)

Compound	$\bar{N}$	$\sigma(\bar{N})$	*Contribution Analysis*
$\mathbf{H_4P_2}$	2.1	0.8	$V(H_1,P_1)$ 24%, $V(P_1,P_2)$ 21%, $C(P_1)$ 20%, $V(P_2)$ 6%
va	2.2	1.0	$V(H_1,P_1)$ 23%, $V(P_1,P_2)$ 19%, $C(P_1)$ 19%, $V(P_2)$ 6%
a	3.4	1.1	$V(H_1,P_1)$ 29%, $C(P_1)$ 21%, $V(P_2)$ 16%
$\mathbf{H_2S_2}$	4.3	1.2	$V(H_1,S_1)$ 34%, $C(S_1)$ 25%, $V(S_1,S_2)$ 24%, $V(S_2)$ 12%
va	4.7	1.2	$V(H_1,S_1)$ 34%, $C(S_1)$ 23%, $V'(S_1)$ 14%, $V(S_2)$ 14%
a	5.5	1.2	$V(H_1,S_1)$ 45%, $C(S_1)$ 30%, $V(S_2)$ 21%
$\mathbf{Cl_2}$	6.4	1.1	$C(Cl_1)$ 42%, $V(Cl_1,Cl_2)$ 26%, $V(Cl_2)$ 30%
va	7.4	1.1	$V(Cl_2)$ 50%, $C(Cl_1)$ 47%
a	7.4	0.9	$V(Cl_2)$ 38%, $C(Cl_1)$ 60%

distance, but remains *greater* than in the neutral parent molecule. The evolution of this contribution upon vertical attachment and relaxation for the two other homodimeric molecules is consistent with the observed charge transfers. In any case, it is always greater in the relaxed anion than in the neutral species.

Let us now discuss the delocalization index of the relaxed radical anions. Starting with the homodimeric compounds, the decrease of $\delta(V(X),V(X))$ as X is taken from Cl to P is consistent with the concomitant decrease of the dissociation energy. It is worth noting the simultaneous decrease of the V(X) spin-integrated densities. If the contribution of the protonated basins were taken into account for the calculation of the delocalization index, the same value would be found for the three radical anions, approximately 0.7, whereas the dissociation energy decreases along the series. This confirms the fundamental role of the lone pairs in the process of electron fluctuation and stabilization of the 3e bond. For heterodimeric compounds, such as H_nXCl^-, the decrease of $\delta(V(X);V(Y))$ from X = Cl to P is due to the increased tendency of the extra electron to locate onto the chlorine atom (as illustrated by the decreasing basin spin densities). In each case (homo- and hetero-dimeric compounds), when X changes from P to Si, the same peculiarity is noted for the delocalization index as it was observed for the others ELF or structural descriptors.

In the framework of VB theory, it is shown that the fluctuation of the electronic charge between the two fragments involved in the bond 2c-3e increases with the resonance energy, i.e., with the overlap of the lone-pair orbitals. It was thus worth considering whether a correlation exists between the electron delocalization as defined in the topological theory of the chemical bond and the dissociation energy of the 3e-bonded radical anions (which is, in a reasonable approximation, proportional to the resonance energy). This correlation was investigated in our original paper on $H_nX\therefore YH_m^-$ radical anions, which addressed compounds isoelectronic to F_2^- and ClF^-, in addition to those compounds isoelectronic to Cl_2^- ones [77]. A linear correlation was obtained if the anions were separated into two groups, depending on whether D_e was smaller or greater than 18 kcal mol^{-1}. It is noteworthy that this value corresponds approximately to the one generally given for the lower bound of the 3e bond dissociation energy (15–20 kcal mol^{-1}). Except for three compounds (H_2PF^-, HSF^- and ClF^-), the most strongly bonded radical anion group consists of all symmetrical systems.

Discussion. Among the investigated radical anions, the chloride dianion Cl_2^- is the prototypical two-center three-electron bonded compound. Its topology is characterized by the absence of the disynaptic V(Cl,Cl) basin, and all valence electron density is located into the monosynaptic basins V(Cl). The morphic number associated with the entire process of electron attachment from the neutral molecule (vertical attachment followed by relaxation) is −1, corresponding to the disappearance of the V(Cl, Cl) basin. The extra electron spin density is equally shared between the two fragments, i.e., between the two V(Cl) basins; the core basins contribute only 8%. A negative covariance is found between the two monosynaptic basins, corresponding to a large positive delocalization index. As the electronegativity of X decreases from X = Cl to P (corresponding to a decrease of the number of lone pairs in the Lewis picture), the greater part of the initial V(X,X) population and of the extra electron density is still transferred into the V(X) basins, but the contribution of the protonated disynaptic V(X,H) increases. As a result, the delocalization index $\delta(V(X),V(X))$ decreases, consistently with the decrease of the dissociation energy of the $X\therefore X^-$ bond. A rupture in this regular evolution arises when X changes from P to Si (a saturated

atom) without available lone pair to absorb electron density. The radical anion presents two newly created monosynaptic basins in place of the V(Si,Si) basin in the bonding region, and two monosynaptic basins are created outside the line joining the two Si atoms but only slightly populated (so that $\Delta\mu = +3$). Only 52% of the integrated spin density is found in these monosynaptic basins, and the delocalization is small (0.10). However, the dissociation energy is on the same order of magnitude as in Cl_2^-, the Si—Si bond length is not much larger than in the neutral and, as already mentioned, the orientation of the fragment does not favor the overlap of the HOMO of the two fragments. Indeed, the bonding in this radical is not purely of the 2c-3e nature. Concerning the heterodimeric radical anions, they all exhibit the typical 2c-3e topology corresponding to $\Delta\mu = -1$ (or $\Delta\mu = 0$ when one of the heavy atoms is Si), except $H_2PSiH_3^-$ which behaves as $H_6Si_2^-$. The ELF descriptors illustrate the weakening of the three-electron bonding character as the difference in electronegativity of the two heavy atoms increases (except when one of the atoms changes from P to Si). The delocalization index of the two compounds that are not purely 3e bonded are found to be small, whereas the integrated spin density of the two monosynaptic basins are well balanced and not negligible compared to the values observed for the other Si-containing radical anions. However, their population is weak and as a consequence the delocalization is smaller.

The SO Radicals

This section is devoted to the investigation of the S···O bond in the anionic, cationic, and neutral radicals, based on structural, energetical, and topological descriptors. A comparison between the performance of different levels of theory BH&HLYP, MP2, and CCSD(T) was presented in the original paper [79] and will not be repeated here. We begin with the $RSOH^-$ radicals, which constitute our reference systems for the S∴O 2c-3e bond. We then investigate the $RR'SOH_2^+$ complexes, which have been considered as 2c-3e bonded systems for a long time. We then finish by examining the RR′SOH complexes, for which the nature of the S···O bond will be established by comparison with the ionic complexes. Concerning the topological ELF analysis, it is noteworthy that we adopt in this section a different point of view than the one used on the three-electron bonded radical anions discussed previously. Previously, we considered the formation of the 2c-3e bond as a result of an electron attachment, whereas now we compare the topology of the complex to those of both isolated fragments (RS and OH^- for the anions, $RR'S^+$ and H_2O for the cations, and RR′S and OH for the neutral). In this context, it is interesting to investigate the global charge transfer from one fragment to another, resulting from the formation of the radical. For the anions, we thus define the variation of population of the sulfur-centered fragment $\Delta\bar{N}(RS)$ as

$$\Delta\bar{N}(RS) = \bar{N}_{comp}(RS) - \bar{N}_{iso}(RS^-) \qquad (12)$$

where $\bar{N}_{comp}(RS)$ is the sum of the basin populations of the RS fragment in the RS∴OH^- 2c-3e bonded complex and $\bar{N}_{iso}(RS^-)$ is the sum of the basin populations of the isolated RS^- fragment ($\Delta\bar{N}(OH) = -\Delta\bar{N}(RS)$). Similar quantities can be calculated for the cation and neutral radicals. The values obtained for all species under scrutiny are gathered in Table 10 and will be discussed together with the other results in the following sections for the anion, cation, and neutral radicals.

Because one of the objectives of this work was to distinguish between a 2c-3e bond or electrostatic interaction, we also define a core valence bifurcation (CVB) index $\vartheta(3e)$, similar to H-bonded complexes as

$$\vartheta(3e) = \eta_{cv} - \eta_{vv}(AB) \qquad (13)$$

where η_{vv} (AB) is the value of the ELF at the saddle connection of the V(A) and V(B) monosynaptic basins of the two fragments and η_{cv} is the lowest value of the ELF for which all the core basins of the composed system are separated from the valence. The CVB determines whether the complex can be considered (negative value) or not (positive value) as a single molecular species. For the H-bonded complexes, it allows distinction between the weak (positive value) and the medium (negative value) H-bonds. As it was suggested for HS∴SH^- by Bergès et al. [54], the CVB indexes of all H_nX∴YH_m^- radical anions are negative. This indicates that these complexes can be considered as single molecular species. More precisely, the values of $\vartheta(3e)$ range from −0.15 to −0.10 and decrease as the difference in electronegativity of the fragments increases. This definition differs from the one given in the original work [79], where we had chosen the opposite value. It is now in better agreement with the CVB index introduced for the H-bonded complexes [96,116].

The $RSOH^-$ Anion Radicals. The corresponding structures are depicted in Fig. 9, together with relevant geometrical data. We note differences with previous results published by Braïda and Hiberty [50] essentially on the angles due to the full geometry relaxation. Bond distances and dissociation energies

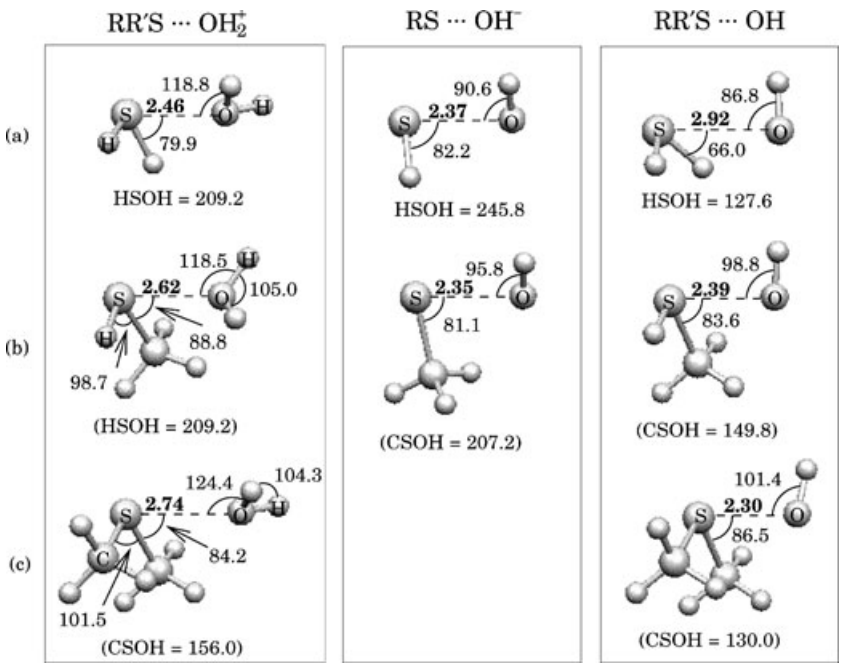

FIGURE 9 Optimized structures for the anionic, cationic, and neutral radicals (adducts) at the CCSD(T)/6-31+G*: (a) R = R′ = H; (b) R = H and R′ = CH_3; (c) R = R′ = CH_3. The nonsubstituted systems have been fully optimized. For the substituted species, only the indicated coordinates have been optimized at the CCSD(T) level, the other ones being kept at their MP2 values (including those between parenthesis). The distances are in angstroms, and the angles are in degrees.

are reported in Table 11. Despite the absence of variations in bond length under substitution, there is a significant increase of the dissociation energy from 20.2 to 25.5 kcal mol^{-1}. This strengthening of the bond, which is expected from the decrease of Δ(EA) (see Table 9), could result from the electron release of the methyl group: indeed, if one considers the formation of RS∴OH^- by the approach of RS:$^-$ and •OH, the substitution takes place on the fragment which bears the lone pair. The ability of RS:$^-$ to transfer electron density toward the hydroxyl fragment may thus be enhanced.

As shown in Fig. 10a, the $HSOH^-$ anion presents the same ELF topology as $H_2S_2^-$, characterized by the absence of disynaptic basin between the two heavy atoms. Under substitution, the V(H,S) basin is replaced by one disynaptic V(S,C) and three protonated disynaptic V(C,H) basins, but no V(S,O) basin is found between the core basins of the S and O atoms. From a global point of view, the formation of the HS∴OH^- anion radical is accompanied by a charge transfer of 0.47*e* from the HS^- to the OH fragment, whereas for CH_3S∴OH^- the charge transfer is equal to 0.53 *e*, as demonstrated by the variations of the gross population of the RS fragment displayed in Table 10. Since the basins involved in this charge transfer are mainly monosynaptic basins of the interacting atoms, the populations, $\bar{N}$, and the integrated spin densities, $\langle S_z \rangle$, of the V(O) and V(S) basins, as well as the delocalization index

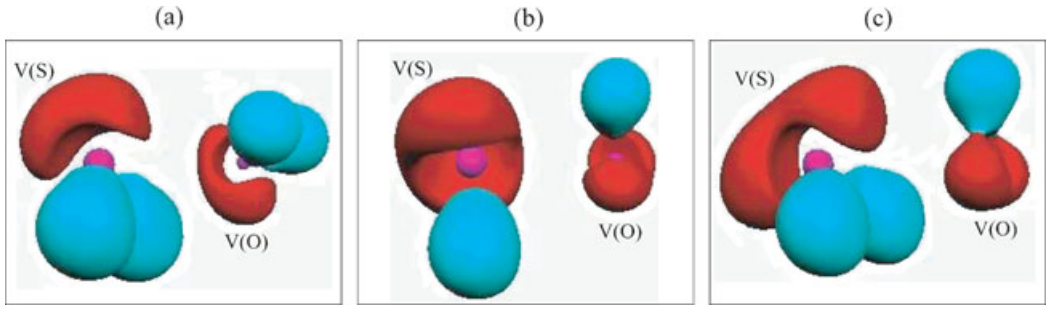

FIGURE 10 ELF = 0.8 isosurfaces for (a) $HSOH^-$, (b) $H_2SOH_2^+$, and (c) H_2SOH.

TABLE 9 Electron Affinities (EA) and Ionization Potentials (IP) of the Fragments and Their Difference (in eV)

RSOH$^-$	*EA(RS)*	*EA(OH)*	Δ*(EA)*
$HSOH^-$	2.31[a]	1.83[b]	0.48
CH_3SOH^-	1.87[c]	1.83[b]	0.04
$RR'SOH_2^+$	IP(H_2O)	IP(RR′S)	Δ (IP)
$H_2SOH_2^+$	12.65[d]	10.46[e]	1.19
$HCH_3SOH_2^+$	12.65[d]	9.45[f]	3.20
$(CH_3)_2SOH_2^+$	12.65[d]	8.69[g]	4.04
RRR′OH	IP(RR′S)	EA(OH)	IP–EA
H_2SOH	10.46[e]	1.83[b]	8.63
HCH_3SOH	9.45[f]	1.83[b]	7.62
$(CH_3)_2SOH$	8.69[g]	1.83[b]	6.86

[a]From Janousek and Brauman [158].
[b]From Smith et al. [159].
[c]From Schwartz et al. [160].
[d]From Snow and Thomas [161].
[e]From Walters and Blais [162].
[f] From Nourbakhsh et al. [163].
[g]From Akopyan et al. [164].

δ (V(S),V(O)) are reported in Table 12. Concerning the isolated fragments, the large population of the V(O) basin, associated with a depleted population of the V(O,H) basin (1.67 *e*), reflects the large electronegativity of the oxygen atom, whereas the population of V(S) in HS^- is in better agreement with the three lone pairs of its Lewis structure. The V(S) population increases by 0.06 *e* in CH_3S^- because of the electron-releasing character of the CH_3 substituent. It is noteworthy that the $\langle S_z \rangle$ value of V(O) corresponds to 84% of the spin density, the missing 16% is distributed among V(H,O) (11%) and C(O) (5%) basins. When $HS^{\cdot\cdot}OH^-$ is forming, the V(S) population decreases by 0.49 *e* whereas the V(O) population increases by 0.45 *e*. Taking into account a slight increase of the V(H,S) population from 1.80 to 1.85 *e*, and neglecting the variations of the core basin populations, we recover the previously mentioned charge transfer of approximately 0.45 *e*, which occurs from the V(S) to the V(O) basin. This results in a quasi-equal sharing of extra electron density and therefore of the spin density among the lone pairs of the two fragments, the V(O) basin being only slightly preferred. As a result of this quasi-uniform distribution of spin density among the two moieties, a large value of the delocalization index δ(V(S), V(O)) is found between the two monosynaptic basins V(S) and V(O). Indeed values of δ around 0.6 have been found for $H_nX^{\cdot\cdot}YH_m^-$ 3e-bonded radical anions, the largest one being obtained for the homonuclear complex $Cl^{\cdot\cdot}Cl^-$, with $\delta = 0.7$. Finally, the negative value of ϑ(3e), −0.13, shows that the complex can be considered as a single molecule. The investigation of the substitution of H by CH_3 on the sulfur atom leads to the following remarks:

1. The V(S) population remains unchanged contrary to the V(O) population which is enhanced by 0.09 *e*. The electron-releasing character of the

TABLE 10 Variation of the Total Basin Population of the Sulfur-Centered Fragment with Respect to the Isolated Fragment, for the Anionic, Cationic, and Neutral Radicals

	$HSOH^-$	CH_3SOH^-	
$\Delta(\bar{N})$(RS)	−0.47	−0.53	
	$H_2SOH_2^+$	$HCH_3SOH_2^+$	$(CH_3)_2SOH_2^+$
$\Delta(\bar{N})$(RR′S)	0.15	0.04	0.03
	H_2SOH	HCH_3SOH	$(CH_3)_2SOH$
$\Delta(\bar{N})$(RR′S)	−0.05	−0.21	−0.29

TABLE 11 Structural and Energetical Parameters of the Anion, Cation, and Neutral Radicals

	This Work		*From Literature*	
Species	R_e	D_e	R_e	D_e
$HSOH^-$	2.37	20.2	2.38[a]	
CH_3SOH^-	2.35	25.5	2.35[a]	
$H_2SOH_2^+$	2.46	22.4	2.42[b]	23.7[b]
			2.46[c]	21.7[c]
			2.437[d]	
			2.454[e]	
				23.8[f]
$HCH_3SOH_2^+$	2.62	18.3		
$(CH_3)_2SOH_2^+$	2.74	15.7	2.88[g]	16.8[g]
H_2SOH	2.92	3.4	2.517[h]	0.2[h]
			2.7702[i]	3.09[j]
HCH_3SOH	2.39	5.0	2.393[h]	2.9[h]
$(CH_3)_2SOH$	2.30	8.4	2.326[h]	7.4[h]
			2.047[k]	9.3[k]
				8.7[l]
			2.3645[m]	7.57[n]

R_e: S–O equilibrium distance in angstroms (Å).
D_e: Dissociation energy of the complex (see text) in kilocalories per mole (kcal mol^{-1}).
The geometry optimizations and the calculations of the dissociation energy have been carried out using the standard 6-31+G* basis. Symmetric species have been optimized within C_s symmetry.
[a]CCSD(T)/6-31+G(d) [50].
[b]BHLYP/6-31++G(d,p) [72].
[c]MP2/6-31++G(d,p) [72].
[d]MP2/6-311G(2d,p) [53].
[e]QCISD/6-311G(2d,p) [53].
[f] MP2/6-31G(d) [3].
[g]HF/6-31G(d) [165].
[h]B3LYP/cc-pVTZ (G2 method) [151].
[i]CCSD(T)/aug-cc-pV(D+*d*)Z [148].
[j] CCSD(T)/augcc-pV(5+*d*)Z//CCSD(T)/aug-cc-pV(D+*d*)Z [148].
[k]MP2/6-31+G(2d) [68].
[l]QCISD(T)/6-31+G(2d)//MP2/6-31+G(2d) [68].
[m]BH&HLYP/aug-cc-pV(D+*d*)Z [148].
[n]CCSD(T)/aug-cc-pV(5+*d*)Z//MP2/aug-cc-pV(D+*d*)Z (the S—O bond length was fixed to 2.3 Å) [148].

TABLE 12 Topological Parameters of the Anion, Cation, and Neutral Radicals and Their Fragments (BHLYP/6-31+G* Single Point Energy Calculation at the CCSD(T)/6-31+G* Geometry)

	V(S)		*V(O)*			
	$\bar{N}$	$\langle(S_z)\rangle$	$\bar{N}$	$\langle(S_z)\rangle$	$\delta_{V(S),V(O)}$	$\vartheta(3e)$
OH			5.28	0.42		
HS^-	6.12					
CH_3S^-	6.18					
$HSOH^-$	5.61	0.21	5.73	0.23	0.58	−0.13
CH_3SOH^-	5.62	0.24	5.82	0.20	0.54	−0.14
OH_2			4.71			
H_2S^+	2.94	0.34				
HCH_3S^+	3.08	0.34				
$(CH_3)_2S^+$	3.19	0.33				
$H_2SOH_2^+$	3.07	0.30	4.45	0.06	0.22	−0.06
$HCH_3SOH_2^+$	3.08	0.31	4.60	0.02	0.12	0.02
$(CH_3)_2SOH_2^+$	3.17	0.32	4.61	0.02	0.10	0.04
H_2S	4.32					
HCH_3S	4.38					
$(CH_3)_2S$	4.46					
H_2SOH	4.26	0.02	5.31	0.40	0.12	0.07
HCH_3SOH	4.05	0.10	5.45	0.32	0.38	−0.07
$(CH_3)_2SOH$	4.00	0.13	5.52	0.28	0.48	−0.13

Population ($\bar{N}$), integrated spin density ($\langle S_z\rangle$) of the monosynaptic basins V(S) and V(O), index of delocalization between these two basins, $\delta_{V(S),V(O)}$, and 3e CVB index, ϑ(3e).

methyl group results in a greater electron transfer from the sulfur atom to the more electronegative oxygen atom. Taking into account the slight increase of the V(S,C) population (from 1.59 to 1.63 *e*), we recover the previously mentioned value of 0.53 *e*. This greater transfer might explain the stabilization of the anion under substitution.

2. The integrated spin densities remain quasi-equally shared among V(S) and V(O), which means that both VB structures of the following resonance (14):

$$RS:^- \cdot OH \longleftrightarrow RS^\cdot \; :OH^- \qquad (14)$$

are nearly equi-probable. Small variations of δ(V(S),V(O)) and ϑ(3e) confirm that the SO bond has the same nature as in the nonsubstituted complex.

In conclusion, the topological ELF-based descriptors obtained for the $RSOH^-$ anion radicals are very similar to those obtained for $H_2S_2^-$ and corroborates the existence of a S∴O bond, consistently with the low values of Δ(EA).

The RR′SOH$_2^+$ Cation Radicals. The corresponding structures are depicted in Fig. 9, together with pertinent geometrical data. The bond distance in the nonsubstituted complex is on the same order of magnitude as in $HSOH^-$ but conversely to the anionic case, it increases by a large amount upon substitution (by 0.16 Å from $H_2SOH_2^+$ to $HCH_3SOH_2^+$ and by 0.12 Å from $HCH_3SOH_2^+$ to $(CH_3)_2SOH_2^+$). Moreover, though the ∠HSO or ∠CSO valence angles are similar to the ones obtained for the radical anions, the ∠HOS angles are much larger, ranging from about 118°–124°, which does not favor an efficient overlap of the lone pairs of the two interacting fragments. Concomitantly with the increase of the S···O distance, the dissociation energy decreases by methyl substitution. This was expected from the increase of Δ(IP), as shown in Table 9. Furthermore, these values are very large as compared to the Δ(EA) of the anions and should not favor a resonance as (1). Similarly as in the anionic case, the weakening of the bond could also be understood by the electron releasing of the methyl group; however, the effect is reversed because the methyl substitution does not take place on the fragment which bears the lone pair. The comparison with previously published results (Table 11) shows that the bond energy of the nonsubstituted system, as the equilibrium structure, is weakly dependent on the chosen method/basis set combination. For $(CH_3)_2SOH_2^+$, where the HF/6-31G(d) dissociation energy is surprisingly correct, the bond length is overestimated. These results do not correspond to the expected performances of the HF method on 2c-3e complexes which are to provide qualitatively correct geometry and largely underestimated bond energy [56]. Finally, though the bond lengths and energies are consistent with what is expected for 2c-3e bonded radical cations, several indicators, as large Δ(IP) or large valence angles, make the 2c-3e nature of the S···O bond in the $RR'SOH_2^+$ complexes questionable.

The ELF isosurface, displayed for $H_2SOH_2^+$ in Fig. 10b, illustrates once more the absence of disynaptic V(S,O) basin. The same topology is observed for the S···O bond in the substituted systems. As shown by Table 10, the formation of the $H_2SOH_2^+$ radical gives rise to a global charge transfer of 0.15 *e*

TABLE 13 Localization ($\langle S_z\rangle$) and Delocalization (δ) Topological Parameters, as well as the CVB Index for the $H_2XYH_2^+$ Cation Radicals (X,Y = S,O). $\delta_{X,Y}$ Quantifies the Electron Delocalization between all the Basins of the H_2X^+ and the H_2Y Moieties

$H_2XYH_2^+$	$\langle S_z\rangle_{V(X)}$	$\langle S_z\rangle_{V(Y)}$	$\delta_{V(X),V(Y)}$	$\delta_{X,Y}$	$\vartheta(3e)$
$H_2S{\cdots}OH_2^+$	0.30	0.06	0.22	0.40	−0.06
$H_2O\therefore OH_2^+$	0.17	0.17	0.28	0.56	−0.18
$H_2S\therefore SH_2^+$	0.19	0.19	0.36	0.64	−0.20

from the H_2O to the H_2S^+ fragment, whereas this transfer is nearly nonexistent for the substituted systems. The data in Table 12 bring to light in more detail the differences between the cationic and anionic cases. What have been said concerning the fragments of the anions complexes is still valid here. In consequence to the formation of the S···O bond in $H_2SOH_2^+$, the V(O) population decreases by 0.26 *e*, among which 0.11 flow into the V(O,H) basins. We thus recover the previously mentioned minor transfer of 0.15 *e*, which occurs from the V(O) to the V(S) basin, namely in the opposite direction to the electron transfer observed in the anions. The fact that the lone pair is provided by the fragment containing the most electronegative atom might explain this weak rearrangement. As a result, the spin density remains essentially localized on the sulfur atom, and that involves a small electron delocalization between the V(S) and V(O) basins, $\delta(V(S), V(O)) = 0.22$, to be compared with about 0.6 in the radical anions. The CVB index is negative, as in the anions, but very close to zero. These topological results are somehow surprising considering the moderate value of the Δ(IP) index. It is thus interesting to compare the topological parameters of $H_2SOH_2^+$ with the equivalent ones in the typical 2c-3e bonded radical cations $H_2O\therefore OH_2^+$ and $H_2S\therefore SH_2^+$. Because of the large number of protonated basins in these three cations, a better picture of the electron delocalization is obtained by considering a global δ(X, Y) index, where X and Y, respectively, represent all the basins of the H_2X^+ and H_2Y fragments. For $H_2SOH_2^+$, the electron delocalization remains rather small (δ(S, O) = 0.40), as shown in Table 13. For $H_2O\therefore OH_2^+$ and $H_2S\therefore SH_2^+$, though the delocalization between the monosynaptic basins alone remains moderate the δ(O, O) and δ(S, S) values, as well as the ϑ(3e) ones, corroborates the 2c-3e nature of the O∴O and S∴S bonds. This is not the case for the S···O bond. Our conclusions, based on a topological approach, also agree with the results of Maity [72], who investigated the nature of the bonding in the radical cation complexes $H_nX\cdots YH_m^+$ by a population-based localization procedure applied to the highest doubly occupied molecular orbital. Here, it was demonstrated that, for $H_2SOH_2^+$ and some other dissymmetric cations, there was no orbital overlap, contrary to all the symmetric species.

The substitution amplifies the localization of the extra electron in the V(S) basin, and consequently still lowers the delocalization index. This was expected from the increase of Δ(IP). Finally, ϑ(3e) becomes positive (though very close to zero), which means that in $HCH_3SOH_2^+$ and $(CH_3)_2SOH_2^+$ the two fragments keep their individuality. Therefore, the 2c-3e type interaction, even in $H_2S\cdots OH_2^+$, is only a minor contribution of the bonding, which should be best described by an electrostatic (dipole–dipole) interaction, this latter contribution increasing with the substitutions. We have now to our disposal some structural and topological data for the 2c-3e S∴O interaction in the radical anion complexes, and for the mainly electrostatic interaction S···O in the radical cation complexes. So, we will investigate the nature of the S···O bond in the neutral radical complexes.

The RR′SOH Neutral Radicals. First, one notices that H_2SOH presents very specific features with respect to the anionic and cationic radicals, because the S···O distance is surprisingly large. It is interesting to compare its structure, depicted in Fig. 9, with those of $HSOH^-$ and $H_2SOH_2^+$: in both latter species, the interaction is mainly between S and O atoms that point toward each other, whereas in the neutral one the hydrogen atoms of the H_2S fragment are directed toward the oxygen of the hydroxyl group ($\angle HSO = 66.0^\circ$). The reason for this could be that this complex is stabilized by a hydrogen bond or van der Waals interaction and not by a 2c-3e S∴O bond. This effect was noticed earlier when comparing the radical anion $HS\therefore HS^-$ to its protonated derivative H_3S_2 [54]. Concomitantly with this large bond distance the dissociation energy is very low, around 3 kcal mol^{-1}.

Second, after one substitution the S···O distance dramatically shrinks, which might indicate a change in the nature of the bond. For both substituted species, many similarities occur between the neutral and anionic radicals. Nevertheless the D_es remain rather low. If we focus our attention on the relation to the experimental data, (see Table 9) we notice that the IP – EA values are larger than the Δ(IP) ones and much larger than the Δ(EA). Thus, at first glance, the situation does not seem very favorable for the formation of a three-electron bond between RR′S and the OH· radical. These large IP – EA values for the RR′SOH radicals may explain the small values of D_e. However, McKee et al. have characterized 2c-3e bonded systems formed by addition between the Cl· radical and nitrogen bases, for which the IP – EA index reaches 6.5 eV [69]. This is not so far from the lowest value (6.9 eV) obtained for $(CH_3)_2SOH$. By substitution D_e increases up to 8.4 kcal mol^{-1}, as expected from the diminution of IP – EA.

Our results for the most studied disubstituted radical are in good agreement with the recent ones obtained by Uchimaru et al. [148], who have confirmed that the S—O bond in this adduct is considerably shorter than in H_2S-OH, and with the first ones of McKee [68]. However, they are somewhat

contradictory with those of Tureček [149,150] and of Wang and Zhang [151]. Whatever method was used, we always obtained 2c-3e type structures, whereas Tureček and Wang and Zhang found different structures depending of the calculation method (see the original paper for the complete discussion [79]). Let us now compare our results on the monosubstituted and nonsubstituted radicals with the 2c-3e structures of Wang and Zhang using the B3LYP functional. The energy and geometry of the monosubstituted radical are close to our CCSD(T) results, as for the disubstituted radical. However, for H_2SOH, Wang and Zhang have found a very weakly bonded structure ($D_e =$ 0.2 kcal mol^{-1}) the SO bond length being 2.517 Å, which is far from our result discussed previously. It must be noted that, even after full optimization at the CCSD(T)/6-311++G(3df,2pd) level, we still obtain a large SO bond length of 2.83 Å, which is in agreement with the recently published value of Uchimaru et al. [148].

The topological results will help us to characterize the nature of the S···O bond in the neutral radicals. Still, there is no localization domain associated with any V(S,O) basin, as shown in Fig. 10c for the simplest H_2SOH. For the quantitative analysis, we must differentiate the nonsubstituted and substituted species, as it was noted for the structural and energetical results. As shown by Table 10, H_2SOH behaves as the substituted radical cations, since there is nearly no charge transfer between the monosynaptic basins. The detailed analysis (see Table 12) shows that the V(O) and V(S) populations are not modified when the S···O bond is created. Consequently, the electron remains mainly localized into the V(O) basin as indicated by the $\langle S_z \rangle$ value of 0.4. The low-delocalization index and positive $\vartheta(3e)$ definitively corroborates the electrostatic nature of the S···O bond, as in the substituted radical cations. In return, the topological parameters of the substituted species show several similarities with those of the anion radicals. As shown by Table 10, there is a nonnegligible charge transfer from the RCH_3S to the OH fragment in the substituted radicals, increasing from 0.21 e in HCH_3SOH to 0.29 e in $(CH_3)_2SOH$. From the population analysis of Table 12, it can be deduced that the charge transfer mainly occurs from the V(S) to the V(O) basin (there is a discrepancy between the global charge transfer and the variations of the basin populations, because of the flow of population to the V(H,S) basin and to the V(S,C) one(s)). As a consequence of this greater charge transfer, the $\langle S_z \rangle$ value of the V(S) basin decreases to 0.28 in the disubstituted radical. Also, the balancing of the spin density gives rise to an increase of the delocalization index, up to 0.48 in $(CH_3)_2S\therefore OH$. The CVB index becomes negative upon substitution, and its value for $(CH_3)_2S\therefore OH$ is the same as in the anions. It is noteworthy that the evolution of the topological features under substitution is consistent with the decrease of the IP – EA index, reported in Table 9. Finally, these topological results bring to light the intermediate nature of the S···O bond in the substituted radicals: it is an interaction essentially electrostatic in HCH_3SOH but 2c-3e bonded in $(CH_3)_2S\therefore OH$.

Conclusion

A review of the abundant literature on the 2c-3e bonding has been presented, showing the importance of these peculiar type of interaction in numerous fields related to radical chemistry. Some molecules proposed by Pauling as candidates for 2c-3e bounded complexes have been studied in the framework of the ELF topological approach. The topological descriptions obtained for the rare gas dimer cations are in agreement with the details provided by the VB theory. However, concerning the neutral radicals NO, OF, and ClO_2, only the nitric oxide can be considered as partially 2c-3e bonded, as shown by the analysis of the basin populations and of the covariance matrix elements. The process of electron attachment on H_nXYH_m molecules and some prototypical complexes containing the SO bond, either with a 2c-3e character or of the electrostatic type, have been investigated in the framework of the ELF topological approach. From these studies, four ELF-based signatures of the two-center three-electron bonding have been elaborated, which are the following:

1. There is no disynaptic V(X,Y) basin associated with a pure X∴Y bond. It should be noted that this result is in agreement with the valence bond description of 2c-3e bonding. In other words, the topology of 2c-3e bonded complexes is composed of the union of the basins of the isolated fragments. Since the same pattern is obtained for all systems formed without electron-pair sharing, as ionic and hydrogen-bonded complexes, some other rules are required to characterize the 2c-3e bond.
2. Two-center three-electron bonded complexes have negative CVB indices, which mean that they can be considered as single molecular species. Typical values of $\vartheta(3e)$ for homonuclear X∴X bonds are around −0.15 decreasing in absolute value as the difference in electronegativity of the fragments increases.

3. The extra electron density (and consequently the spin density) is mainly localized within the monosynaptic basins V(X) and V(Y). Strongest 2c-3e bonds are characterized by well-balanced sharing of the spin density between the two moieties, and thus occur for two identical fragments. As far as 2c-3e bonded radical anions are concerned, it is noteworthy that the electron cloud reorganization following electron attachment can be somehow hampered by conservation of the geometry (vertical processes). The removal of this constraint by relaxation enables the disappearance of the bonding basin and the localization of the spin density into the lone-pair regions.
4. The electron fluctuation between the two fragments, which is a central phenomenon in three-electron bonds, occurs mainly between the lone pairs of two heteroatoms X and Y. It can be quantified by the delocalization index δ(V(X), V(Y)), which is maximal (around 0.7) for homonuclear X∴X bonds and decreases as the difference in electronegativity of the fragments increases (lower values are around 0.4). Though the CVB index is useful to distinguish 3e bonds from ionic or hydrogen bonds, the delocalization index is more robust and can be considered as the proper topological fingerprint for 2c-3e bonding.

Finally, it is worth comparing the topological pictures obtained for the 2c-3e bonding and for the CS electron-pair bonding [152]. This latter type of bonding has been recently revisited by Shaik et al. [146] into the framework of both VB theory and topological analysis of ELF. In CS-bonded (closed-shell) species, whose prototype is the F_2 molecule, the fluctuation of the electron-pair density plays a dominant role. In VB theory, this is manifested by large covalent–ionic resonance energy. In ELF, this is revealed by a depleted basin population with large variance and negative covariance, corresponding to superposition of promolecular densities such as $F^+F^- \leftrightarrow F^-F^+$. Thus, apart from the absence of bonding population, and the open-shell character of the 3e-bonded species, the same physical picture is obtained for these two peculiar types of bonding.

ACKNOWLEDGMENTS

This work has been supported by the CNRS (UMR7616) and the Université Pierre et Marie Curie. We are indebted to Alain Sevin, Hilaire Chevreau, and Jacqueline Bergés for their contribution to previously published work on this subject, to B. Braïda for fruitful discussions, and to P. Reinhardt and Alexander C. Kollias for their critical reading of the manuscript.

REFERENCES

[1] Pauling, L. J Am Chem Soc 1931, 53, 3225.
[2] Pauling, L. The Nature of the Chemical Bond; Cornell University Press: Ithaca, NY, 1948.
[3] Clark, T. J Am Chem Soc 1988, 110, 1672.
[4] Neuman, E. W. J Chem Phys 1934, 2, 31.
[5] Brockway, L. O. Proc Natl Acad Sci USA 1933, 19, 303.
[6] Asmus, K. D. Acc Chem Res 1979, 12, 436.
[7] Göbl, M.; Bonifaičić, M.; Asmus, K. D. J Am Chem Soc 1984, 106, 5984.
[8] Chaudhri, S. A.; Mohan, H.; Anklam, E.; Asmus, K.-D. J Chem Soc, Perkin Trans 2 1996, 383–390.
[9] Bobrowski, K.; Hug, G. L.; Schöneich, D. J Phys Chem A 1998, 102, 10512.
[10] Kishore, K.; Aced, E. A.; Asmus, K. D. J Phys Chem A 2000, 104, 9646.
[11] Asmus, K. D. Nukleonika 2000, 45, 3.
[12] de Visser, S. P.; de Konig, L. J.; Nibbering, N. M. M. J Am Chem Soc 1998, 120, 1517.
[13] de Visser, S. P.; Bieckelhaupt, F. M.; de Konig, L. J.; Nibbering, N. M. M. Int J Mass Spectrom 1998, 179/180, 43.
[14] Nichols, L. S.; Illies, A. J. J Am Chem Soc 1999, 121, 9176.
[15] King, J. E.; Illies, A. J. J Phys Chem A 2004, 108, 3581.
[16] Wakamiya, A.; Nishinaga, T.; Komatsu, K. J Am Chem Soc 2002, 124, 15038.
[17] Asmus, K. D. In Sulfur-Centered Reactive Intermediates in Chemistry and Biology; Chatgilialoglu, C.; Asmus, K. D. (Eds.); Plenum Press: New York, 1990; pp. 155–172.
[18] Glass, R. S. In Sulfur-Centered Reactive Intermediates in Chemistry and Biology. Chatgilialoglu, C.; Asmus, K. D. (Eds.); Plenum Press: New York, 1990; p. 213.
[19] Gilbert, B. C. In Sulfur-Centered Reactive Intermediates in Chemistry and Biology. Chatgilialoglu, C.; Asmus, K. D. (Eds.); Plenum Press: New York; 1990; p. 135.
[20] Bonifacic, M.; Schöneich, G. L. H. C. J. J Phys Chem A 2000, 104, 1240.
[21] Lmoumène, C. E. H.; Conte, D.; Jacquot, J. P.; Houée-Levin, C. Biochemistry 2000, 39, 9295.
[22] Schöneich, C. Biochim Biophys Acta 2005, 1703, 111.
[23] Yashiro, H.; White, R. C.; Yurkovskaya, A. V.; Forbes, M. D. E. J Phys Chem A 2005, 109, 5855.
[24] Abu-Raqabah, A.; Symons, M. C. R. J Chem Soc Faraday Trans 1990, 86, 3293 and references therein.
[25] Symons, M. C. R.; Bowman, R. J. J Chem Soc, Perkin Trans 2 1990, 975.
[26] Shanker, U. R.; Symons, M. C. R.; Wyatt, J. L.; Bowman, R. J. J Chem Soc, Faraday Trans 2 1993, 89, 1199.
[27] Sevilla, M. D.; Summerfield, S.; Eliezer, I.; Rak, J.; Symons, M. C. R. J Phys Chem A 1997, 101, 2910.

[28] Chateauneuf, J. E. Chem Commun 1998, (19), 2099–2100.
[29] Gauduel, Y.; Launay, T.; Hallou, A. J Phys Chem A 2002, 106, 1727.
[30] Balkowski, G.; Szemik-Hojniak, A.; van Stokkum, I. H. M.; Zhang, H.; Buma, W. J. J Phys Chem A 2005, 109, 3535.
[31] Scaiano, J. C.; García, S.; García, H. Tetrahedron Lett. 1997, 38, 5929.
[32] Lakkaraju, P. S.; Shen, K.; Roth, H. D.; García, H. J Phys Chem A 1998, 103, 7381.
[33] Sono, M.; Roach, M. P.; Coulter, E. D.; Dawson, J. H. Chem Rev 1996, 96, 2841 and references therein.
[34] Shaik, S.; Filatov, M.; Schröder, D.; Schwartz, H. Chem Eur J 1998, 4, 193.
[35] Ogliaro, F.; Harris, N.; Cohen, S.; de Visser, M. F. S. P.; Shaik, S. J Am Chem Soc 2000, 122, 8977 and references therein.
[36] Symons, M. C. R.; Rhodes, C.; Reid, I. Magn Reson Chem 2000, 38, 823.
[37] Goez, M.; Rozwadowski, J.; Marciniak, B. Angew Chem Int Ed 1998, 37, 628.
[38] Pogocki, D.; Ghezzo-Schöneich, E.; Schöneich, C. J Phys Chem B 2001, 105, 1250.
[39] Gill, P. M. W.; Radom, L. J Am Chem Soc 1988, 110, 4931.
[40] Yokoi, H.; Hatta, A.; Ishiguro, K.; Sawaki, Y. J Am Chem Soc 1998, 120, 12728.
[41] Knops-Gerrits, P.-P.; Jacobs, P. A.; Fukuoka, A.; Ichakawa, M.; Faglioni, F.; Goddard, W. A., III. J Mol Catal A: Chem 2001, 166, 3.
[42] Kasai, P. H. J Phys Chem A 2002, 106, 83.
[43] Kasai, P. H.; Himmel, H.-J. J Phys Chem A 2002, 106, 6765.
[44] Boyd, D. C.; Connelly, N. G.; Herbosa, G. G.; Hill, M. G.; Mann, K.; Mealli, C.; Orpen, A. G.; Richardson, K. E.; Rieger, P. H. Inorg Chem 1994, 33, 960.
[45] Connelly, N. G.; Hayward, O. D.; Klangsinsirikul, P.; Rieger, P. H. Chem Commun 2000, 11, 963.
[46] Chen, E. C. M.; Dojahn, J. G.; Wentworth, W. E. J Phys Chem A 1997, 101, 3088.
[47] Chen, E. C. M.; Chen, E. S. Chem Phys Lett 1998, 293, 491.
[48] Chen, E. C. M.; Wentworth, W. E. J Phys Chem 1985, 89, 4099.
[49] Dojhan, J. G.; Chen, E. C.; Wentworth, W. E. J Phys Chem 1996, 100, 9649.
[50] Braïda, B.; Hiberty, P. J Phys Chem A 2000, 104, 4618.
[51] McKee, M. L. J Phys Chem 1992, 96, 1675.
[52] Bickelhaupt, F. M.; Diefenbach, A.; de Visser, S. P.; de Koning, L. J.; Nibbering, N. N. M. J Phys Chem A 1998, 102, 9549.
[53] Carmichael, I. Nukleonika 2000, 41, 11.
[54] Bergès, J.; Fuster, F.; Silvi, B.; Jacquot, J.; Houée-Levin, C. Nukleonika 2000, 45, 23.
[55] Braïda, B.; Hiberty, P. C. J Phys Chem A 2003, 107, 4741.
[56] Hiberty, P. C.; Humbel, S.; Danovich, D.; Shaik, S. J Am Chem Soc 1995, 117, 9003.
[57] Hiberty, P. C.; Humbel, S.; Archirel, P. J Phys Chem 1994, 98, 11697–11704.
[58] Braïda, B.; Hiberty, P.; Savin, A. J Phys Chem A 1998, 102, 7872.
[59] Sodupe, M.; Bertran, J.; Guez Santiago, L.-R.; Baerends, E. J. J Phys Chem A 1999, 103, 166.
[60] Chermette, H.; Ciofini, I.; Mariotti, F.; Daul, C. J Chem Phys 2001, 115, 11068.
[61] Grüning, M.; Gritsenko, O. V.; van Gisbergen, S. J. A.; Baerends, E. J. J Phys Chem A 2001, 105, 9211.
[62] Ghanty, T. K.; Gosh, S. K. J Phys Chem A 2002, 106, 11815.
[63] Becke, A. D. J Chem Phys 1993, 98, 1372.
[64] Jaramillo, J.; Scuseria, G. E. J Chem Phys 2003, 118, 1068.
[65] Gräfenstein, J.; Kraka, E.; Cremer, D. Phys Chem Chem Phys 2004, 6, 1096.
[66] Gerber, I. C.; Ángyán, J. G. Chem Phys Lett 2005, 405, 100.
[67] Humbel, S. Ph.D. thesis, Université Paris-Sud, Orsay, France, 1995.
[68] McKee, M. L. J Phys Chem 1993, 97, 10971.
[69] McKee, M. L.; Nicolaides, A.; Radom, L. J Am Chem Soc 1996, 118, 10571.
[70] Braïda, B.; Lauvergnet, D.; Hiberty, P. J Chem Phys 2001, 115, 90.
[71] Hiberty, P. C.; Berthe-Gaujac, N. J Phys Chem A 1998, 102, 3169.
[72] Maity, D. K. J Phys Chem A 2002, 106, 5716.
[73] Braïda, B.; Hazbroucq, S.; Hiberty, P. C. J Am Chem Soc 2002, 124, 2371.
[74] Dézarnaud-Dandine, C.; Sevin, A. J Am Chem Soc 1996, 18, 4427.
[75] Braïda, B.; Thogersen, L.; Wu, W.; Hiberty, P. C. J Am Chem Soc 2002, 124, 11781.
[76] Braïda, B.; Hiberty, P. C. J Am Chem Soc 2004, 126, 14890.
[77] Fourré, I.; Silvi, B.; Sevin, A.; Chevreau, H. J Phys Chem A 2002, 106, 2561.
[78] Humbel, S.; Hiberty, P. C. J Mol Struct 1998, 424, 57.
[79] Fourré, I.; Bergès, J. J Phys Chem A 2004, 108, 898.
[80] Humbel, S.; Demachy, I.; Hiberty, P. C. Chem Phys Lett 1995, 247, 126.
[81] Humbel, S.; Côte, I.; Hoffmann, N.; Bouquant, J. J Am Chem Soc 1999, 121, 5507.
[82] Humbel, S.; Hoffmann, N.; Côte, I.; Bouquant, J. Chem Eur J 2000, 6, 1592.
[83] Pogocki, D.; Schöneich, C. Chem Res Toxicol 2002, 15, 408.
[84] Pogocki, D.; Schöneich, C. J Org Chem 2002, 67, 1526.
[85] Pogocki, D.; Serdiuk, K.; Schöneich, C. J Phys Chem A 2003, 107, 7032.
[86] Huang, M. L.; Rauk, A. J Phys Chem A 2004, 108, 6222.
[87] Becke, A. D.; Edgecombe, K. E. J Chem Phys 1990, 92, 5397.
[88] Bader, R. F. W. Atoms in Molecules: A Quantum Theory; Oxford University Press: Oxford, UK; 1990.
[89] Silvi, B.; Savin, A. Nature 1994, 371, 683.
[90] Noury, S.; Colonna, F.; Savin, A.; Silvi, B. J Mol Struct 1998, 450, 59.
[91] Silvi, B. J Mol Struct 2002, 614, 3.
[92] Silvi, B. J Phys Chem A 2003, 107, 3081.
[93] Silvi, B. Phys Chem Chem Phys 2004, 6, 256.
[94] Savin, A. J Mol Struct (Theochem) 2005, 727, 127.

[95] Silvi, B.; Fourré, I.; Alikhani, M. E. Monatsh Chem 2005, 136, 855.
[96] Fuster, F.; Silvi, B. Theor Chem Acc 2000, 104, 13.
[97] Fourré, I.; Silvi, B.; Chaquin, P.; Sevin, A. J Comput Chem 1990, 93, 2992.
[98] Beltrán, A.; Andrés, J.; Noury, S.; Silvi, B. J Phys Chem A 1999, 103, 3078.
[99] Llusar, R.; Beltrán, A.; Andrés, J.; Noury, S.; Silvi, B. J Comput Chem 1999, 20, 1517.
[100] Berski, S.; Silvi, B.; Latajka, Z.; Leszczyński, J. J Chem Phys 1999, 111, 2542.
[101] Krokidis, X.; Moriarty, N. W.; William A. Lester, J.; Frenklach, M. Chem Phys Lett 1999, 314, 534–542.
[102] Chevreau, H.; Sevin, A. Chem Phys Lett 2001, 322, 9.
[103] Silvi, B.; Gatti, C. J Phys Chem A 2000, 104, 947.
[104] Fuster, F.; Sevin, A.; Silvi, B. J Phys Chem A 2000, 104, 852.
[105] Fuster, F.; Sevin, A.; Silvi, B. J Comput Chem 2000, 21, 509.
[106] Fuster, F.; Silvi, B. Chem Phys 2000, 252, 279.
[107] Chesnut, D. B.; Bartolotti, L. J. Chem Phys 2000, 253, 1.
[108] Chamarro, E.; Santos, J. C.; Gómez, B.; Contreras, R.; Fuentealba, P. J Chem Phys 2001, 114, 23.
[109] Boily, J. J Phys Chem A 2002, 106, 4718.
[110] Alikhani, M.; Silvi, B. Phys Chem Chem Phys 2003, 5, 2494.
[111] Gillespie, R. J.; Noury, S.; Pilme, J.; Silvi, B. Inorg Chem 2004, 43, 3248.
[112] Berski, S.; Gutsev, G. L.; Mochena, M. D.; Andres, J. J Phys Chem A 2004, 108, 6025.
[113] Bil, A.; Latajka, Z. Chem Phys 2004, 303, 43.
[114] Fuster, F.; Dézarnaud-Dandine, C.; Chevreau, H.; Sevin, A. Phys Chem Chem Phys 2004, 6, 3228.
[115] Chaquin, P.; Scemama, A. Chem Phys Lett 2004, 394, 244.
[116] Alikhani, M.; Fuster, F.; Silvi, B. Struct Chem 2005, 16, 203.
[117] Cárdenas, C.; Chamorro, E.; Notario, R. J Phys Chem A 2005, 109, 4352.
[118] Lavanant, H.; Fressigné, C.; Simonnet-Jégat, C.; Dessapt, R.; Mallard, A.; Sécheresse, F.; Sellierc, N. Int J Mass Spectrom 2005, 243, 205.
[119] Chesnut, D. B.; Crumbliss, A. L. Chem Phys 2005, 315, 53.
[120] Poater, J.; Duran, M.; Solà, M.; Silvi, B. Chem Rev 2005, 105, 3911.
[121] del Carmen Michelini, M.; Russo, N.; Alikhani, M. E.; Silvi, B. J Comput Chem 2005, 26, 1284.
[122] Andrés, J.; Berski, S.; Feliz, M.; Llusar, R.; Sensato, F.; Silvi, B. C R Chim 2005, 8, 1400.
[123] Ormeci, A.; Rosner, H. Z Kristallogr 2004, 219, 370.
[124] Gatti, C. Z Kristallogr 2005, 220, 399.
[125] Krokidis, X.; Noury, S.; Silvi, B. J Phys Chem A 1997, 101, 7277.
[126] Krokidis, X.; Silvi, B.; Dézarnaud-Dandine, C.; Sevin, A. New J Chem 1998, 22, 1341.
[127] Berski, S.; Andres, J.; Silvi, B.; Domingo, L. R. J Phys Chem A 2003, 107, 6014.
[128] Santos, J. C.; Andrés, J.; Aizman, A.; Fuentealba, P. J Chem Theory Comput 2005, 1, 83.
[129] Polo, V.; Andrés, J. J Comput Chem 2005, 26, 1427.
[130] Lewis, G. N. J Am Chem Soc 1916, 38, 762.
[131] Lewis, G. N. Valence and the Structure of Atoms and Molecules; Dover: New York, 1966.
[132] Abraham, R.; Marsden, J. E. Dynamics and the Geometry of Behavior; Addison-Wesley: Reading, MA, 1992.
[133] Abraham, R.; Marsden, J. E. Foundations of Mechanics; Addison-Wesley: Reading, MA, 1994.
[134] Dobson, J. F. J Chem Phys 1991, 94, 4328.
[135] Savin, A.; Jepsen, O.; Flad, J.; Andersen, O. K.; Preuss, H.; von Schnering, H. G. Angew Chem Int Ed Engl 1992, 31, 187.
[136] Häussermann, U.; Wengert, S.; Nesper, R. Angew Chem, Int Ed Engl. 1994, 33, 2069.
[137] McWeeny, R. Methods of Molecular Quantum Mechanics, 2nd. ed.; Academic Press: London, 1992.
[138] Fradera, X.; Austen, M. A.; Bader, R. F. W. J Phys Chem A 1999, 103, 304.
[139] Mezey, P. G. Can J Chem 1993, 72, 928.
[140] Frisch, M. J.; Trucks, G. W.; Schlegel, H. B.; Gill, P. M. W.; Johnson, B. G.; Robb, M. A.; Cheeseman, J. R.; Keith, T.; Petersson, G. A.; Montgomery, J. A.; Raghavachari, K.; Al-Laham, M. A.; Zakrzewski, V. G.; Ortiz, J. V.; Foresman, J. B.; Cioslowski, J.; Stefanov, B. B.; Nanayakkara, A.; Challacombe, M.; Peng, C. Y.; Ayala, P. Y.; Chen, W.; Wong, M. W.; Andres, J. L.; Replogle, E. S.; Gomperts, R.; Martin, R. L.; Fox, D. J.; Binkley, J. S.; Defrees, D. J.; Baker, J.; Stewart, J. P.; Head-Gordon, M.; Gonzalez, C.; Pople, J. A. Gaussian 94, Revision D.4; Gaussian, Inc.: Pittsburgh, PA, 1995.
[141] Frisch, M. J.; Trucks, G. W.; Schlegel, H. B.; Scuseria, G. E.; Robb, M. A.; Cheeseman, J. R.; Zakrzewski, V. G.; Montgomery, J. A., Jr.; Stratmann, R. E.; Burant, J. C.; Dapprich, S.; Millam, J. M.; Daniels, A. D.; Kudin, K. N.; Strain, M. C.; Farkas, O.; Tomasi, J.; Barone, V.; Cossi, M.; Cammi, R.; Mennucci, B.; Pomelli, C.; Adamo, C.; Clifford, S.; Ochterski, J.; Petersson, G. A.; Ayala, P. Y.; Cui, Q.; Morokuma, K.; Malick, D. K.; Rabuck, A. D.; Raghavachari, K.; Foresman, J. B.; Cioslowski, J.; Ortiz, J. V.; Baboul, A. G.; Stefanov, B. B.; Liu, G.; Liashenko, A.; Piskorz, P.; Komaromi, I.; Gomperts, R.; Martin, R. L.; Fox, D. J.; Keith, T.; Al-Laham, M. A.; Peng, C. Y.; Nanayakkara, A.; Challacombe, M.; Gill, P. M. W.; Johnson, B.; Chen, W.; Wong, M. W.; Andres, J. L.; Gonzalez, C.; Head-Gordon, M.; Replogle, E. S.; Pople, J. A. Gaussian 98, Revision A.9; Gaussian, Inc.: Pittsburgh, PA, 1998.
[142] Frisch, M. J.; Trucks, G. W.; Schlegel, H. B.; Scuseria, G. E.; Robb, M. A.; Cheeseman, J. R.; Montgomery, J. A., Jr.; Vreven, T.; Kudin, K. N.; Burant, J. C.; Millam, J. M.; Iyengar, S. S.; Tomasi, J.; Barone, V.; Mennucci, B.; Cossi, M.; Scalmani, G.; Rega, N.; Petersson, G. A.; Nakatsuji, H.; Hada, M.; Ehara, M.; Toyota, K.; Fukuda, R.; Hasegawa, J.; Ishida, M.; Nakajima, T.; Honda, Y.; Kitao, O.; Nakai, H.; Klene, M.; Li, X.; Knox, J. E.; Hratchian, H. P.; Cross, J. B.; Bakken, V.; Adamo, C.; Jaramillo, J.; Gomperts, R.; Stratmann, R. E.; Yazyev, O.; Austin, A. J.; Cammi, R.; Pomelli, C.; Ochterski, J. W.; Ayala, P. Y.; Morokuma, K.; Voth, G. A.; Salvador, P.; Dannenberg, J. J.; Zakrzewski, V. G.; Dapprich, S.; Daniels, A. D.; Strain, M. C.; Farkas,

O.; Malick, D. K.; Rabuck, A. D.; Raghavachari, K.; Foresman, J. B.; Ortiz, J. V.; Cui, Q.; Baboul, A. G.; Clifford, S.; Cioslowski, J.; Stefanov, B. B.; Liu, G.; Liashenko, A.; Piskorz, P.; Komaromi, I.; Martin, R. L.; Fox, D. J.; Keith, T.; Al-Laham, M. A.; Peng, C. Y.; Nanayakkara, A.; Challacombe, M.; Gill, P. M. W.; Johnson, B.; Chen, W.; Wong, M. W.; Gonzalez, C.; Pople, J. A. Gaussian 03, Revision B.02; Gaussian, Inc.: Wallingford, CT, 2004.

[143] Noury, S.; Krokidis, X.; Fuster, F.; Silvi, B. Topmod package, 1997.

[144] Noury, S.; Krokidis, X.; Fuster, F.; Silvi, B. Comput Chem 1999, 23, 597.

[145] Flükiger, P.; Lüthi, H.; Portmann, S.; Weber, J. Molekel 4.0; Swiss Center for Scientific Computing: Manno, Switzerland, 2000.

[146] Shaik, S.; Danovich, D.; Silvi, B.; Lauvergnat, D.; Hiberty, P. Chem Eur J, 2005, 11, 6358.

[147] The lone-pair basins of each given center have been merged because we are only interested by their fluctuation as a whole.

[148] Uchimaru, T.; Tsuzuki, S.; Sugie, M.; Tokuhashi, K.; Sekiya, A. Chem Phys Lett 2005, 408, 216.

[149] Tureček, F. J Phys Chem 1994, 98, 3701.

[150] Tureček, F. Collect Czech Chem Commun 2000, 65, 455.

[151] Wang, L.; Zhang, J. J Mol Struct 2001, 543, 167.

[152] Shaik, S.; Maître, P.; Sini, G.; Hiberty, P. C. J Am Chem Soc 1992, 114, 7861.

[153] Huber, K. P.; Herzberg, G. Molecular Spectra and Molecular Structure IV: Constants of Diatomic Molecules; Van Nostrand Reinhold: New York, 1979.

[154] Dehmer, P. H.; Pratt, S. T. In Photophysics and Photochemistry in the Vacuum Ultraviolet; Glynn, S. P.; Findley, G. L.; Hueber, R. H. (Eds.); D. Reidel: Dordrecht, Holland, 1985, 260.

[155] Horn, E. F.; Dickey, F. P. J Chem Phys 1964, 41, 1614.

[156] O'Hare, P. A. G.; Wahl, A. C. J Chem Phys 1970, 53, 2469.

[157] Kuchitsu, K. (Ed.). Landolt-Bornstein, Numerical Data Functional Relationships in Science and Technology: Group II, Atomic and Molecular Physics; Springer-Verlag: Berlin, 1992, Vol. 21.

[158] Janousek, B. K.; Brauman, J. Phys Rev A 1980, 23, 1673.

[159] Smith, J.; Kim, J.; Lineberger, W. Phys Rev A 1997, 55, 2036.

[160] Schwartz, R.; Davico, G.; Lineberger, W. J Electron Spectrosc Relat Phenom 2000, 108, 163.

[161] Snow, K.; Thomas, T. Int J Mass Spectrom Ion Processes 1990, 96, 49.

[162] Walters, E.; Blais, N. J Chem Phys 1984, 80, 3501.

[163] Nourbakhsh, S.; Norwood, K.; Yin, H.-M.; Liao, C.-L.; Ng, C. Y. J Chem Phys 1991, 95, 946.

[164] Akopyan, M.; Sergeev, Y.; Vilesov, F. High Energy Chem 1970, 4, 265; also in Khim Yys Energ 1970, 4, 305 (in Russian).

[165] Clark, T. In Sulfur-Centered Reactive Intermediates in Chemistry and Biology; Chatgilialoglu, C.; Asmus, K. D. (Eds.); Plenum Press: New York, 1990, pp. 13–18.